OPEN ACCESS
IOP Publishing | Songshan Lake Materials Laboratory
Materials Futures
Mater. Futures 2 (2023) 042102 (18pp)
https://doi.org/10.1088/2752-5724/ace3de

Topical Review

Review of regulating Zn^{2+} solvation structures in aqueous zinc-ion batteries

Wanyao Zhang[1,3], Yufang Chen[1,*], Hongjing Gao[1], Wei Xie[1], Peng Gao[2], Chunman Zheng[1,*] and Peitao Xiao[1,3,*]

[1] College of Aerospace Science and Engineering, National University of Defense Technology, Changsha, Hunan 410073, People's Republic of China
[2] College of Materials Science and Engineering, Hunan Joint International Laboratory of Advanced Materials and Technology of Clean Energy, Hunan Province Key Laboratory for Advanced Carbon Materials and Applied Technology, Hunan University, Changsha 410082, People's Republic of China

E-mail: Chenyufang@nudt.edu.cn, zhengchunman@nudt.edu.cn, xpt_fdu@126.com and xiaopt@nudt.edu.cn

Received 7 June 2023, revised 1 July 2023
Accepted for publication 4 July 2023
Published 4 August 2023

Abstract

Aqueous zinc-ion batteries, due to their high power density, intrinsic safety, low cost, and environmental benign, have attracted tremendous attentions recently. However, their application is severely plagued by the inferior energy density and short cycling life, which was mainly ascribed to zinc dendrites, and interfacial side reactions, narrow potential window induced by water decomposition, all of which are highly related with the Zn^{2+} solvation structures in the aqueous electrolytes. Therefore, in this review, we comprehensively summarized the recent development of strategies of regulating Zn^{2+} solvation structures, specially, the effect of zinc salts, nonaqueous co-solvents, and functional additives on the Zn^{2+} solvation structures and the corresponding electrochemical performance of aqueous zinc-ion batteries. Moreover, future perspectives focused on the challenges and possible solutions for design and commercialization of aqueous electrolytes with unique solvation structures are provided.

Keywords: solvation structure, aqueous electrolyte, zinc-ion batteries, zinc dendrites

1. Introduction

Lithium-ion batteries using non-aqueous electrolytes have been dominated the market since 1990s. However, their further application is severely impeded due to their high cost, limited sources, and notorious safety issues [1–3]. Aqueous metal ion batteries, due to their low cost, intrinsic safety, environmental benign, and high power density, have been widely investigated recently, among which zinc ion batteries (ZIBs) have attracted increasing attentions because of the low redox potential (−0.76 V vs standard hydrogen electrode) and high volumetric capacity (5860 mAh cm^{-3}) of Zn [4–7].

However, their practical application has been plagued by low energy density and poor cycling stability, which was induced by inferior structural stability of cathode, narrow stable potential window, zinc dendrites or corrosions, side reactions on the electrode-electrolyte interfaces [8, 9]. To address these issues, researchers have done tremendous efforts to design various types of cathodes, functional electrolytes, current collectors, and artificial solid-electrolyte interphases (SEI), and investigate the fundamental electrochemical mechanisms. For instance, vanadium/Mn-based

[3] W Z and P X contribute equally to this work.
[*] Authors to whom any correspondence should be addressed.

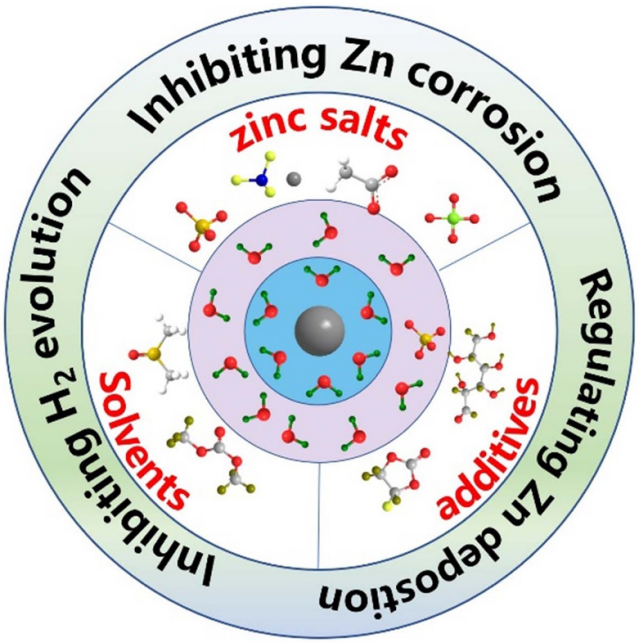

Figure 1. Schematical illustration of the contents in the review.

materials, metal-organic frameworks, organic molecules are widely explored as the cathodes in ZIBs, and great progresses have been made in improving the specific capacity and cycling stability of cathodes [4, 10–12].

Electrolytes, as the media to transport Zn^{2+} and directly contact with both anode and cathode, not only have a crucial effect on electrochemical kinetics, but also play a key role in broadening the electrochemical stable potential windows (ESPWs), suppression of zinc dendrites and corrosions, and inhabitation of water decomposition and side reactions, highly affecting the overall electrochemical performance, including energy/power density and cycling life of ZIBs [13–15]. Moreover, compared with other strategies such as designing electrodes, current collectors, and artificial electrode-electrolyte interphases with sophisticated structures or components, electrolyte engineering is facile and easy for industrial application. Therefore, various types of aqueous electrolytes, including highly concentrated electrolytes (HCEs), hybrid electrolytes with organic solvents or polymers as cosolvents, electrolyte with functional additives have been widely investigated [16–21].

In the conventional aqueous electrolytes for ZIBs, zinc salts dissolve into water, forming hydrate Zn^{2+}, $[Zn(H_2O)_6]^{2+}$. Because of the strong cation-solvent (Zn^{2+}–H_2O) interactions, only water, instead of anion, existed in the solvation shell of Zn^{2+}, leading to the prior reduction of water and increase of PH near the anode, which further resulting into the Zn corrosion and formation of by-products. Moreover, the inferior kinetics at the SEI accelerates the formation of zinc dendrites, leading to the rapid capacity fading of ZIBs. Thus, regulation of Zn^{2+} solvation structure is significantly important to overcome the challenges in ZIBs.

In this review, we mainly focus on summarization of recent development of strategies to regulate the Zn^{2+} solvation structures and their effects on the corresponding Zn-electrolyte interfacial electrochemical performances in aqueous ZIBs. Specifically, the effect of zinc salts (concentration and salt types), co-solvents (organic solvents and polymers), and functional additives (salts, organic additives, inorganic additives) on the solvation structures and the electrochemical performances (figure 1).

2. Zinc salts

In the aqueous electrolyte, the solvation structures are determined by the relative interaction between cation-anion and cation-solvent. If the overall interaction of cation-anion is stronger than that of cation-solvent, the anions can partially replace the solvent in the solvation structure. There are usually two ways to manipulating the Zn^{2+} solvation structures in ZIBs: adoption of different zinc salts or change the concentration of zinc salts.

2.1. Zinc salts with different anions

Various zinc salts have been investigated as the solute in aqueous ZIBs, as shown in figure 2. Since these zinc salts have the same cation, the components and their structures of the counteranions have great effects on the physiochemical property and solvation structures of the aqueous ZIBs. For example, in inorganic zinc salt, ZnF_2, due to the strong electronegativity of F, ZnF_2 hardly dissolves into water, while $ZnCl_2$ has a high solubility due to the large radius and relative weak electronegativity of Cl^-. Therefore, systemically investigation of the effect of different zinc salts on the solvation structures and the corresponding electrochemical performances [22]. In this section, we only discuss the effect of zinc salts with concentration $\leqslant$2 M (mol l^{-1}) on the Zn^{2+} solvation structures to avoid repetition with the next section.

Zhang *et al* investigated the effect of different zinc salts on the ESPWs and the Zn stripping/platting kinetics, as shown in figure 3. Electrolytes with $ZnCl_2$ and $Zn(NO_3)_2$ show poor electrochemical stability with ESPWs no more than 1.5 V vs. Zn^{2+}/Zn, exhibiting poor compatibility with Zn anode and inferior oxidation resistance (figures 3(a) and (b)), while these with $Zn(OTF)_2$ and $ZnSO_4$ deliver ESPWs larger than 2 V vs. Zn^{2+}/Zn (figures 3(c) and (d)). Moreover, compared that using $ZnSO_4$, cells using $Zn(OTF)_2$ delivered both enhanced reversibility and improved kinetics during Zn stripping/platting processes, which was ascribed to that the bulky anion ($CF_3SO_3^-$) with large size decreased the water in the Zn^{2+} solvation structures and fastened the desolvation of Zn^{2+} [23]. This phenomenon was also observed in electrolyte with $Zn(TFSI)_2$ by Peng *et al* [24] Different from $ZnCl_2$, electrolytes with 1 M $Zn(ClO_4)_2$ show anodic stability up to 2.4 V and an average coulombic efficiency (CE) of 99%, which is better than those of electrolytes with $ZnSO_4$ and $Zn(OAC)_2$ [25]. Moreover, in the aqueous low-concentrated electrolytes with different salts ($ZnSO_4$, $ZnCl_2$, $Zn(ClO_4)_2$, $Zn(TFSI)_2$, and $Zn(OTF)_2$), similar solvation structures with Zn^{2+} coordinated with five or six water molecules are expected, while other water molecules form a

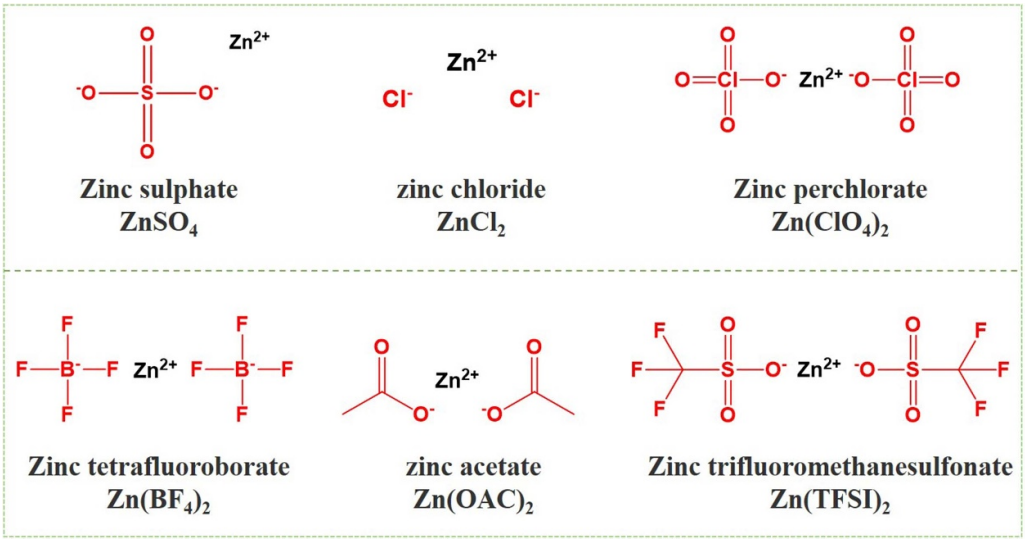

Figure 2. Molecular structures of various zinc salts.

network via hydrogen bonding, leading to narrow ESPWs, side interfacial reactions, and formation of zinc dendrites [26–29]. Although various aqueous electrolytes using different zinc salts with low concentration have been investigated, they still cannot meet the requirement of aqueous ZIBs. Therefore, aqueous electrolytes using zinc salts with high concentration have been explored.

2.2. HCEs

By increasing the concentration of zinc salts, the overall interaction of cation-anion increases while that of cation-water decreases, facilitating the desolvation of Zn^{2+}, thus inhibiting the formation of zinc dendrites. Meanwhile, improving the salt concentration decreases the number of water molecule in the Zn^{2+} solvation structure, simultaneously inhibiting the formation of hydroxyl OH^- and the following byproducts. Moreover, HCEs can significantly broaden ESPWs, which has been proven in various electrochemical systems [30]. For example, 30 M $ZnCl_2$ in water was used in aqueous ZIBs to improve the inferior electrochemical performance in conventional electrolytes [31].

Wang *et al* designed an aqueous electrolyte composed of 1 m $Zn(TFSI)_2$ and 20 m LiTFSI for ZIBs (1 m = 1 mol kg^{-1}). In this HCE (or water in salt), Zn^{2+} was mainly coordinated with $TFSI^-$ instead of water, forming a solvation sheath of Zn $(TFSI)_n$, and leading to an anion-derive interphases, which effectively inhibited the H_2 evolution and facilitated Zn stripping/platting. As a result, the Zn||Pt cells exhibited an average CE of >99.7% after more than 200 cycles at 1 mA cm^{-2}, and Zn||Zn symmetric cells shown stable cycling stability for more than 500 cycle at 0.2 mA cm^{-2} without formation of ZnO byproduct [32]. Similarly, Wan *et al* investigated the effect of HCEs, composed of 1 M $Zn(OTF)_2$ and 21 M LiTFSI in water, on the electrochemical performance of aqueous ZIBs, and it was found that the oxygen evolution (begin at 2.6 V) was significantly suppressed at high voltage due to the unique solvation structures in HCEs [33]. Similarly, a HCE consisted of 1 M $Zn(OTF)_2$ and 15 M LiTFSI in water was used to suppressed water decomposition and cathode dissolution at high cut-off voltage, resulting into a capacity retention of 82.3% after 2000 cycles [34].

Later, Zhao designed a 'water-in-deep eutectic solvent' electrolytes composed of water and urea/LiTFSI/$Zn(TFSI)_2$, which have similar solvation structures with those of HCEs and all water participated into the deep eutectic solvent's internet network without free water molecules. As a result, the electrolyte delivered a wide ESPW of >2.5 V vs Zn^{2+}/Zn and enhanced Zn stripping/platting stability with cycle life of >2000 h at 0.1 mA cm^{-2}. Zn/$LiMn_2O_4$ battery using this electrolyte exhibited a capacity retention of >90% after 300 cycles at 0.1 C [35]. A novel hydrate deep eutectic electrolyte composed of sulfolane (SL) and $Zn(ClO_4)_2 \cdot 6H_2O$ was designed by Lin *et al* for aqueous ZIBs operated under low temperature. The unique solvation structures of this novel hydrate deep eutectic electrolyte facilitated Zn^{2+} diffusion and deposition, and reduced water reactivity, leading to ZIBs with organic cathodes operated at −30 °C with excellent cycling stability [36]. Binary hydrate melt electrolyte composed of $ZnCl_2$ and $Zn(OAC)_2$ was also designed for aqueous ZIBs, which effectively expelled water molecules from Zn^{2+} solvation structures, significantly suppressing the water decomposition, Zn corrosion [37]. Ionic liquids are also used as the salts for HCEs in ZIBs. For instance, electrolytes composed of 4 m $Zn(TFSI)_2$ + 4 m $P_{444(2O1)}$ -TFSI in water were explored by Ma *et al*, and they found that the addition of $P_{444(2O1)}$ -TFSI changed the solvation structure of Zn^{2+}, leading to polymeric-species containing and fluorine-rich SEI, which enabled Zn||Cu cells with a CE of 99.9% and Zn||Zn cells with excellent cycling stability even at current density of 2.5 mA cm^{-2} [38].

In 2021, Zhu designed another novel HCE by addition of $NaClO_4$ into $Zn(ClO_4)_2$-based electrolyte, forming 0.5 m

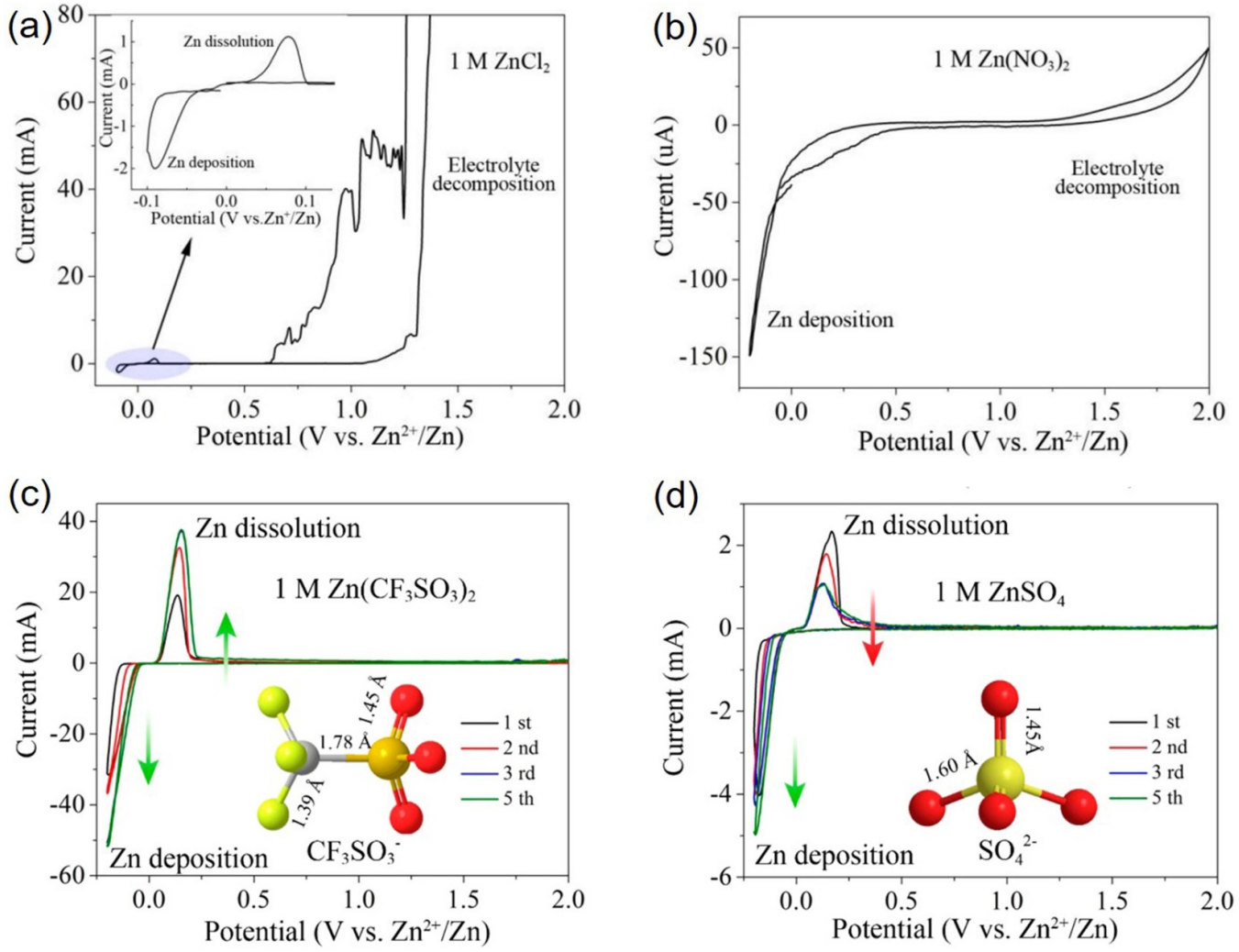

Figure 3. Cyclic voltage curves of Zn||Zn symmetric cells using (a) 1 M $ZnCl_2$, (b) 1 M $Zn(NO_3)_2$, (c) 1 M $Zn(OTF)_2$, (d) 1 M $ZnSO_4$ aqueous electrolytes between −0.2 and 2.0 V at a scanning rate of 0.5 mV s^{-1}. Reprinted with permission from [23]. Copyright (2016) American Chemical Society.

$Zn(ClO_4)_2$ + 18 m $NaClO_4$ aqueous electrolyte. In the dilute electrolyte composed of 0.5 m $Zn(ClO_4)_2$ in water, Zn^{2+} coordinated with six water molecules (figure 4(a)), in accordance with that in other dilute aqueous electrolytes. With the addition of $NaClO_4$, ClO_4^- appeared in the solvation shell of Zn^{2+} due to the stronger Zn^{2+}– ClO_4^- affinity compared with that of Na^+– ClO_4^- (figure 4(b)). ClO_4^- dominated the solvation sheath of Zn^{2+} without water molecule when further increasing concentration of $NaClO_4$ (figure 4(c)), which was also demonstrated the shift of ^{35}Cl nuclear magnetic resonance (NMR) signal in figure 4(d). Due to the change of Zn^{2+} solvation structures, a ClO_4^- derived Cl-containing SEI was successfully constructed on the surface of Zn, leading to an average CE of 98.2% in Zn||Ti cells at 0.4 mA cm^{-2} over 100 cycles and enhanced cycling stability of Zn||Zn cells with 1200 h at 0.2 mA cm^{-2} [26].

Recently, MOF-based super-concentrated electrolytes were proposed by Zhou's group and applied them into aqueous ZIBs. For instance, they designed a ZIF67-based electrolyte with a concentration of 2 M $ZnSO_4$ in water. In the tradition HCEs, with the increases of zinc salt concentration, anion gradually replaced the water molecules in the Zn^{2+} solvation structures, forming solvent separated ion pair and contact ion pair (CIP), the ratio of which are 56% and 44% in the saturated $ZnSO_4$ electrolyte (∼3.3 M, figure 4(e)). In the ZIF67-based electrolyte, even at a concentration of 2 M, a unique solvation structure was formed in which Zn^{2+} and SO_4^{2-} are coordinated more closely due to the size constraint of small pore size of ZIF67, as shown in figure 4(f). This unique solvation structure can effectively suppress the side reactions and promote Zn plating, as a result, Zn||Zn symmetric cells delivered an enhanced cycling life of near 3000 h at 0.5 mA cm^{-2} with compact and dendrite-free deposition (figures 4(g)–(j)) [39]. Similar strategies was also adopted using zeolite molecular sieve instead of ZIF67 by the same group, and significantly enhanced electrochemical performance was also obtained: symmetric Zn||Zn cells delivered a ultra-long cycle life of 4765 h at 0.8 mA cm^{-2} with compact Zn deposition, and Zn||VO_2 cells exhibited a capacity retention of 70.3% after 3000 cycles [40].

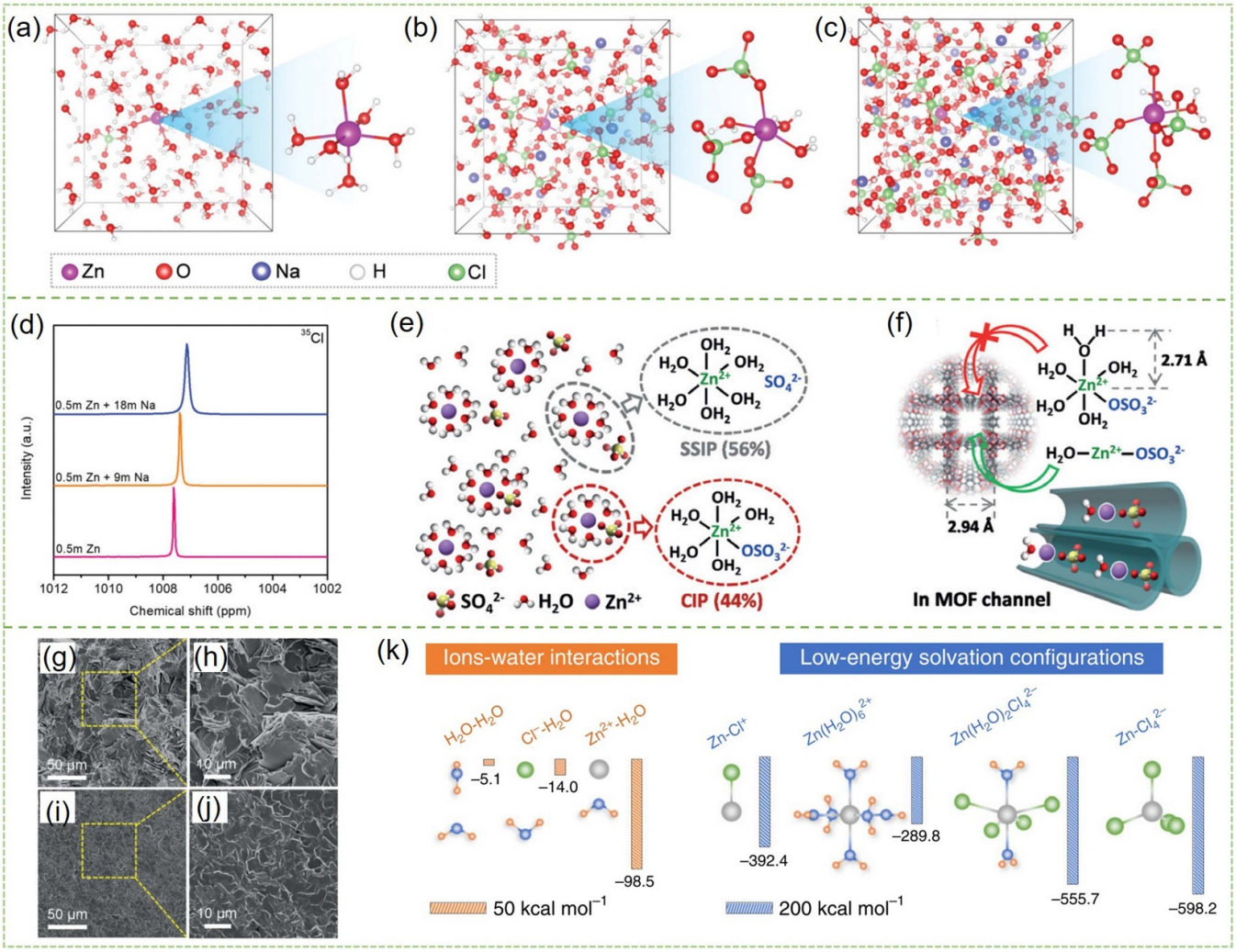

Figure 4. Snapshots of equilibrium trajectories from MD simulation of (a) 0.5 m $Zn(ClO_4)_2$, (b) 0.5 m $Zn(ClO_4)_2$ + 9 m $NaClO_4$, and (c) 0.5 m $Zn(ClO_4)_2$ + 18 m $NaClO_4$. (d) ^{35}Cl NMR of different electrolytes. Reproduced from [26] with permission from the Royal Society of Chemistry. Schematic illustration of Zn^{2+} solvation structures in (e) saturated ZnSO4 electrolytes and (f) MOF-based electrolyte. SEM images of (g), (h) bared Zn and (i), (j) MOF-coated Zn. [39] John Wiley & Sons. [© 2020 Wiley-VCH Verlag GmbH & Co. KGaA, Weinheim]. (k) The calculated formation energy of ions and water. Reproduced from [41]. CC BY 4.0.

Zhang *et al* systemically investigated the concentration of zinc salt ($ZnCl_2$) from dilute (1 M) to highly concentrated (30 M) on the Zn^{2+} solvation structures and their performance under low temperatures. It was found that with increasing concentration of $ZnCl_2$, the ratio and $Zn(H_2O)_6^{2+}$ decreased with the increase of $Zn(H_2O)_2Cl_4^{2-}$; when the concentration was higher than 7.5 M, $ZnCl_4^{2-}$ and polynuclear aggregate appeared and increased with improving salt concentration, which both breaking H-bonds in dilute electrolytes (figure 4(k)). Meanwhile, the solvation structure in 7.5 M $ZnCl_2$ electrolytes shown less ion interaction, depressing the liquid-glass transition, thus leading to better low-temperature performance. Therefore, using 7.5 M $ZnCl_2$ in water, Zn||Cu cells delivered a high CE of 99.52% at −70 °C, Zn||Zn symmetric cells exhibited a cycle life of 450 h at −70 °C, and polyanilineǁZn batteries worked in a wide temperature from −90 to +60 °C with a capacity retention of almost 100% at −70 °C over 2000 cycles [41]. Sun *et al* also investigated an electrolyte of 4 M $Zn(BF_4)_2$ in low-temperature, which enabled Zn||tetrachlorobenzoquinone battery worked at temperature as low as −95 °C since the introduction of BF_4^- into the Zn^{2+} solvation structure could effectively break the H-bonds in dilute electrolyte [42].

Recently, Wang introduced 2, 2, 2-trifluoroethanol (TFE) into highly concentrated aqueous electrolyte (30 M $ZnCl_2$ in water), due to electron withdraw effect of CF_3^- in TFE, H-bonds formed between TFE and water in the solvation structure. As a result, Zn^{2+} solvation structure changed from large cluster in 30 M $ZnCl_2$ in water to smaller clusters with higher ratio of $Zn(H_2O)_2Cl_4^{2-}$, resulting into high CE of 99.74% after 100 cycles in Zn||Cu cells, long cycle life of >4000 h, and excellent cycling stability with a capacity retention of 87.6% after 2000 cycles at 2 A g^{-1} for Zn||(Polyaniline) PANI batteries [43].

Although adoption of HCEs can significantly improve the electrochemical performance, the high concentration of zinc salts inevitable increase the viscosity of electrolyte, exacerbating the electrochemical kinetics and power density of aqueous ZIBs; meanwhile zinc salts with high concentration highly increase the prices of ZIBs, both of which compromise the advantages of aqueous ZIBs such as low cost and high power density.

3. Nonaqueous solvents

In aqueous ZIBs, adoption of water enables batteries with intrinsic safety and excellent ion transport kinetics, which, however, result into structural instability of both cathode and anode, narrow ESPWs, Zn dendrites, and interfacial side reactions [30, 44]. Using nonaqueous solvents as the cosolvent can significantly decreases the numbers of free water and water in the solvation structures, thus effectively alleviating the above issues. In this section, we mainly summarized the effect of nonaqueous solvents, including organic solvents and polymers, on solvation structure/behavior and the corresponding electrochemical performances [11, 45–47].

3.1. Organic solvents

There are usually two types of organic solvents, nonpolar solvents and polar solvents. In order to regulate solvation structures of Zn^{2+}, only polar solvents are investigated. These polar solvents include esters, ethers, amides, alcohols, sulfones or sulfoxides, and other polar solvents.

Propylene carbonate (PC), as the solvent of aqueous electrolyte in ZIB, was investigated by Ming *et al* [48]. Molecule dynamics (MD) simulation demonstrated that in pure electrolyte (1 M $Zn(OTF)_2$ in water), there were only six water molecules in the primary solvation sheath of Zn^{2+}. When the volume ratio of PC increased to 50%, the number of H_2O in primary solvation sheath decreased to 2 (figures 5(a) and (b)), which was further reduced to about 0.5, while more PC and OTF^- dominated the primary solvation structures, when the volume ratio of PC increased to 90%. The variation of solvation structures not only minimized the water, but also leading to the formation of robust anion-derived $ZnCO_3$, ZnF_2-containing SEI. As a result, the hybrid electrolyte (1 M $Zn(OTF)_2$ in water: PC, 1:1) exhibited a wide ESPW of 3.1 V ($-0.6 \sim 2.5$ V), enabling Zn||Cu cells with an average CE of 99.66% after 500 cycles and Zn||Zn cells with a cycling life >1600 h. Zhang *et al* explored dimethyl carbonate (DMC) as the co-solvent in aqueous electrolytes, and found that in hybrid electrolyte (2 M $Zn(OTF)_2$ in water: DMC, 4:1), DMC and OTF^- both appeared in the solvation structures due to the strong interactions between Zn^{2+} and DMC and OTF^-, forming a solvation structure of $Zn^{2+}[H_2O]_{3.9}[DMC]_{0.7}[OTF^-]_{1.4}$, which was different from that in pure aqueous electrolyte, further resulting into a robust organic/inorganic hybrid SEI rich in $ZnCO_3$ and ZnF_2 (figure 5(c)). As a result, an average CE of 99.8% was achieved in Zn||Ti cells after 600 cycles at a high current density of 5 mA cm^{-2}, and Zn||Zn symmetrical cells shown improved cycling stability over 1000 h at 1 mA cm^{-2} without Zn dendrites (figure 5(d)). Triethyl phosphate (TEP), due to its high donor number (DN, 26 kcal mol^{-1}), was investigated by Liu *et al.* By replace 50% of the water with TEP in the aqueous electrolyte, TEP dominated the primary solvation structures, resulting into a robust a robust poly-ZnP_2O_6 and ZnF_2-rich polymeric-inorganic SEI, thus effectively inhibiting water activity and formation of Zn dendrites. As a result, using this electrolyte (0.5 M $Zn(OTF)_2$ in water: TEP, 1:1), Zn||Cu cells exhibited an average CE of 99.5% after 200 cycles, and Zn||V_2O_5 cells maintained 250 mA h g^{-1} after 1000 cycles at a current density of 5 A g^{-1} [49]. Other esters, such as diethyl carbonate (DEC) and trimethyl phosphate (TMP) are widely investigated as the co-solvent in aqueous electrolytes, which show [50–52].

Besides esters, ethers are also investigated as co-solvents in aqueous electrolytes. Du *et al* explored 1,3-dioxolane (DOL) as the co-solvent in aqueous electrolyte of ZIBs, and found that the addition of DOL altered the solvation structures of Zn^{2+}, thus expanding the potential of hydrogen evolution. As a result, Zn||Ti cells with the hybrid electrolytes (1 M $Zn(OTF)_2$ in water: DOL) exhibited excellent stripping/platting reversibility with CE of 98.6% after 300 cycles, and Zn||V_2O_5 cells maintained a high capacity retention of 94% after 1500 cycles [58]. Another linear ether, 1,2-dimethoxyethane (DME) was also adopted in the aqueous electrolytes. As shown in figure 5(e), when the volume ratio of DME increased to 40%, H-bond network was interrupted and solvation structure only with water coordinated with Zn^{2+} changed to that with DME and OTF^-, which further leading to the formation of an organic-inorganic SEI with ZnF_2 and ZnS, effectively inhibiting water-involved side reactions and Zn dendrites. Consequently, high reversibility of Zn||Cu cells with CE of 99.7% over 800 cycles, excellent cycling stability of Zn||Zn symmetric cells with 5000 h at 2.0 mA cm^{-2} were achieved. Moreover, Zn||VOH full cells also shown significantly enhanced cycling stability with capacity retentions of 93.1% and 73.4% after 2000 and 4000 cycles, respectively, at 2 A g^{-1} [54].

Hao *et al* investigated methanol as the anti-solvent in ZIBs, and found that with the volume increasing, methanol firstly interacted with water, breaking the original H-bond network, then gradually enter into the primary sheath of Zn^{2+}, both of which could minimize the water-induced side reactions. As shown in figure 5(f), the addition of methanol effectively expanded the ESPWs and inhibited water decomposition. Zn||Cu cells using 2 M $ZnSO_4$ in water: methanol (1:1 by volume) achieved an average CE of 99.7% after 900 cycles. Moreover, both Zn||Cu cells and Zn||PANI cells using this hybrid electrolyte exhibited enhanced wide-temperature performance [55]. Besides methanol, ethanol, 1,5-pentanediol, glycerol, and ethylene glycol have been widely explored [27, 28, 61–63].

In 2020, dimethyl sulfoxide (DMSO) was used by Cao *et al* to investigate its effects on ZIBs. As schematically shown in figure 5(g), the addition of DMSO not only interrupted the original H-bonds in water, but also appeared in the primary sheath of Zn^{2+}, resulting into SEI with abundant $Zn_{12}(SO_4)_3Cl_3(OH)_{15}\cdot 5H_2O$, $ZnSO_3$, and ZnS. As a result,

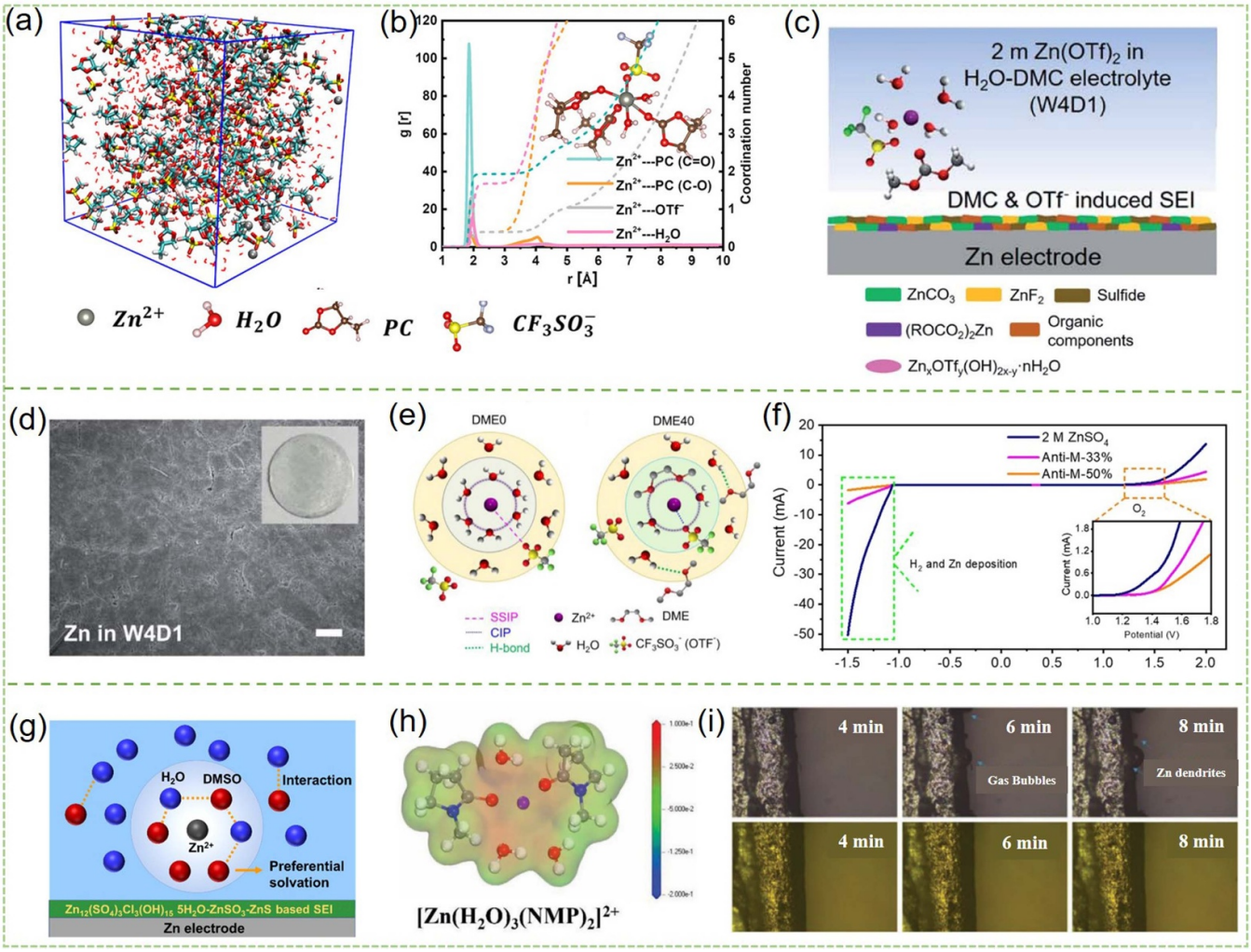

Figure 5. (a) Snapshot of MD simulation of electrolyte composed of 1 M $Zn(OTF)_2$ in water: PC (1:1), and (b) the corresponding radical distribution function. Reprinted with permission from [48]. Copyright (2022) American Chemical Society. (c) Schematic of the SEI and the interfacial chemistry in 2 M $Zn(OTF)_2$ in water: DMC, and (d) SEM of Zn after cycling. Reproduced from [53] with permission from the Royal Society of Chemistry. (e) Schematically illustration of solvation structures in electrolytes with or without DME. Reprinted from [54], Copyright (2022), with permission from Elsevier. (f) LSV curves of different electrolytes [55]. John Wiley & Sons. [© 2021 Wiley-VCH GmbH]. (g) Schematics of solvation structures of $ZnCl_2-H_2O-DMSO$ hybrid electrolyte and SEI. Reprinted with permission from [56]. Copyright (2020) American Chemical Society. (h) Electrostatic potential of solvation structures in DMA-based electrolytes. (i) Optical images of Zn anode in different electrolytes [57]. John Wiley & Sons. [© 2022 Wiley-VCH GmbH].

the $ZnCl_2-H_2O-DMSO$ hybrid electrolyte endowed Zn||Ti cells with a high CE of 99.5% for 400 h, and Zn||MnO2 cells a high capacity retentions of 95.3% after 500 cycles [56]. In 2022, Li *et al* found that N-methyl-2-pyrrolidone (NMP) was effective to regulate the solvation structures of Zn^{2+} (figure 5(h)) and inhibiting Zn dendrites and hydrogen evolution (figure 5(i)). Consequently, using electrolytes composed of 2 M $ZnSO_4$ in water: NMP (1:1 by volume), Zn||Cu cells achieved high average CE of 99.7% after 1000 cycles, Zn||Zn cells exhibited cycling stability of over 500 h at 1 mA cm^{-2}, and Zn/VS_2 full cells delivered an ultralong cycle life with a capacity retention of 99.4% after 2000 cycles, demonstrating the significant effect of NMP on ZIBs [57]. Moreover, other organic solvents, such as tetramethylurea (TMU) [64, 65], N,N-dimethylformamide (DMF) [8], and N, N-dimethyl acetamide (DMA) [66, 67], also show great potentials in improving electrochemical performance of ZIBs, the performances of which have been summarized in table 1.

3.2. Polymers

Besides small organic molecules, polymers with polar functional groups also have significant effects on reshape of the solvation chemistry. Polyethylene glycol (PEG), as a representative polar polymer have been explored. Wu *et al* found that PEG and anions would enter into the solvation structures of Zn^{2+} with increasing the addition of PEG, as shown in figure 6(a) [60]. Moreover, compared with electrolytes with high concentration of zinc salts, addition of PEG significantly reduced the free water in the solvation structures, as shown in figures 6(b)–(d) [59]. Meanwhile, PEG interacted with H_2O, interrupting the original H–bond network. Due to the

Table 1. Typical electrolytes and their effects on electrochemical performance of ZIBs.

Electrolyte	ESPWs (V)	CEs of half cells after cycles (%, cycles)	Cycle life for Zn||Zn cells at different current densities (h, mA cm^{-2})	References
Zn salts				
1 m $Zn(TFSI)_2$ and 20 m LiTFSI in water	—	>99.7, >200	170, 0.2	[32]
$Zn(TFSI)_2$/LiTFSI/ Urea in water	>2.5	96.2, 11	2400, 0.1	[35]
Sulfolane and Zn(ClO4)2 · 6H2O	—	98, 100	800, 0.5	[36]
4 m $Zn(TFSI)_2$ + 4 m $P_{444(2O1)}$ -TFSI in water	2.42	99, –	>800, 1	[38]
0.5 m $Zn(ClO_4)_2$ + 18 m $NaClO_4$	—	98.4, 100	>1200, 0.2	[26]
2 M $ZnSO_4$–ZIF67 in water	—	—	3000, 0.5	[39]
7.5 M $ZnCl_2$ in water	—	99.52 (−70 °C)	450, 0.2 (−70 °C)	[41]
20 mol% TFE into 30 m $ZnCl_2$	>2.4	99.74, 100	>4000, 0.2	[43]
Aqueous solvents				
2 M $Zn(OTF)_2$ in water: DMC (1:4 by volume)	—	99.8, 600	>1000, 1	[53]
1 M $Zn(OTF)_2$ in water: PC (1:1 by volume)	∼3.1	99.66, 500	>1600, –	[48]
0.5 M $Zn(OTF)_2$ in water: TEP (1:1 by volume)	—	99.5, 200	—	[49]
2 m $Zn(OTF)_2$ + 7 m DEC in water	—	99.24%, 400	>3500, 5	[50]
1 M $Zn(OTF)_2$ in water: DOL (1:1 by volume)	—	98.6%, 300	1000, 1	[58]
2 M $Zn(OTF)_2$ in water: DOL (3:2 by volume)	—	99.7%, 800	5000, 2	[54]
2 M $ZnSO_4$ in water: methanol (1:1 by volume)	—	99.7%, 900	—	[55]
1.3 m $ZnCl_2$ in water: DMSO (4.3:1 by volume)	—	99.5, 400	—	[56]
2 M $ZnSO_4$ in water: NMP (1:1 by volume)		99.7, 1000	>500, 1	[57]
2 M $Zn(OTF)_2$ + 0.25 M TMU in water		99.5, 1200	>1500, 5	[64]
2 M $ZnSO_4$ in water: DMA		99.6%, 700	>4500, 1	[66]
2 M $Zn(OTF)_2$ in water: PEG (3:7 by weight)	—	99.7%, 150	—	[59]
1 M $Zn(OTF)_2$ in water: PEG (3:7 by weight)		—	9000, 1	[60]
Functional additives				
2 M $ZnSO_4$ in water with 1vol. % Py	2.68	99.5, 1200	3300, 0.5	[76]
2 M $ZnSO_4$ in water with 0.05 M EDTA	—	98.5, 200	3000, 5	[73]
2 M $ZnSO_4$ in water with 1vol. % FEC	—	99.1, 250	1000, 4	[78]
2 M $ZnSO_4$ in water with 1vol. % SL	—	99.64, 400	1000, 2	[79]
2 M $ZnSO_4$ +0.2 M Mn SO_4 in water with 5% DX	—	99.8, 200	600, 5	[70]
2 M $ZnSO_4$ +5 mM vanillin in water	—	99.8, 800	1000, 1	[71]
3 M $Zn(OTF)_2$ + 1 M urea + 0.3 M LiOAC in water	—	99.7, >1500	600, 4.8	[72]
1 M $ZnSO_4$ +5 mM TU in water	—	98.9, 700	1200, 1	[75]
1 M $ZnSO_4$ +10 mM glucose in water	—	97.2, 200	2000, 1	[77]
2 M $ZnSO_4$ in water with 2% 15-CE-5	—	—	700, 2	[80]
1 M $ZnSO_4$ +0.25 mM PA in water	—	99.4, 225	1200, 1	[81]
1 M $ZnSO_4$ +0.2 M 18C6 in water	—	99.5, 200	2400, 1	[83]
2 M $ZnSO_4$ +50 mM TXA in water	—	99.6, 1000	2000, 1	[84]
3 M $ZnSO_4$ +10 mM TH in water	—	99.5, 200	580, 1	[87]
3 M $Zn(OTF)_2$ in water with 2 vol. % Et_2O	—	—	250, 0.2	[88]
1 M $ZnSO_4$ in water with 0.2 wt % PAM	—	99.65, 1300	—	[29]
1 M $ZnSO_4$ in water with 0.5 wt % SF	—	—	1600, 1	[93]
2 M $ZnSO_4$ in water with 2 mg ml^{-1} silk peptide	—	99.7, 1000	3000, 1	[94]
1 M $ZnSO_4$ in water with 0.2 wt % PEO		99.5%, >600	>110, 1	[92]
2 M $ZnSO_4$ +0.05 mM TBA_2SO_4 in water	—		400, 10	[95]
1 M $ZnSO_4$ +0.05 M TA-Na in water	—	99.3, 1000	1500, 0.5	[96]
1 M $Zn(OTF)_2$ +25 mM $Zn(H_2PO_4)_2$ in water	—	99.4, 400	1200, 1	[97]
7.6 M $ZnCl_2$ + 0.05 M $SnCl_2$ in water	—	99.7, 200	500, 3	[99]
2 M $ZnSO_4$ +0.5 M ims in water	—	—	4000, 10	[101]
2 M $ZnSO_4$ +0.5 M PEA in water		99.75%, 6000	>2000, 1	[89]

reshape of solvation structure, ZnF_2 -rich SEI was successfully constructed, interfacial side reactions and Zn dendrites were highly suppressed. Therefore, as shown in figure 6(e), the addition of PEG highly expanded ESPW of electrolyte. The Zn dendrites and H_2 evolution were also inhibited, as shown in figure 6(f) and (g). As a result, using electrolytes

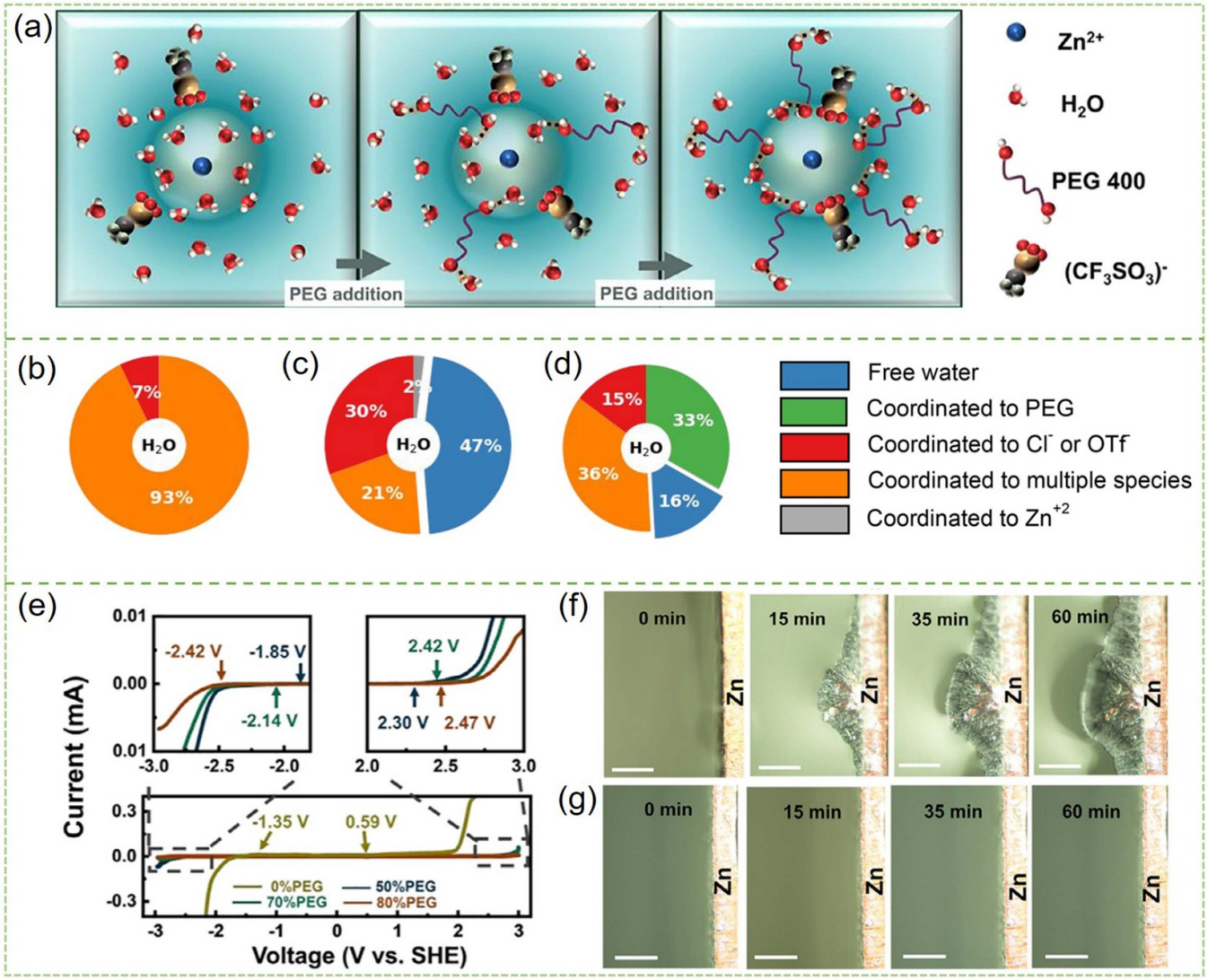

Figure 6. (a) Schematical illustration of evolution of solvation structures with the increase of PEG concentration. Ratios of different complexes in the solvation structures in different electrolytes: (b) 21 M $ZnCl_2$ in water, (c) 4 M $Zn(OTF)_2$ in water, and (d) 2 M $Zn(OTF)_2$ in water/PEG. Reprinted with permission from [59]. Copyright (2022) American Chemical Society. (e) LSV curves in different electrolytes. Optical images of Zn during platting process in (f) 1 M $Zn(OTF)_2$ in water and (g) 1 M $Zn(OTF)_2$ in water/PEG. Reprinted from [60], Copyright (2022), with permission from Elsevier.

composed of 2 M $Zn(OTF)_2$ in water: PEG (3:7 by weight), Zn||Cu cells exhibited an improved CE of 99.7% after 100 cycles; using electrolytes of 1 M $Zn(OTF)_2$ in water: PEG (3:7 by weight), Zn||Zn cells exhibited excellent cycling stability of 9000 h at 1 mA cm^{-2}.

Similar with that in HCEs, addition of co-solvents improves, to some extent, the viscosity, exaggerating the kinetics. Moreover, due to the flammability of most organic or polymer molecules, the intrinsic safety of aqueous electrolyte are compromised. Therefore, decreasing the content of co-solvent while maintaining the overall electrochemical performance is, though challenging.

4. Functional additives

Functional additives, as important component of aqueous electrolyte, play a key role in improving the electrochemical performance with small amount of addition. Besides, since the weight ratio of additives in the electrolyte is very low (usually $\leqslant$5 wt%), the addition of functional additives usually has little effect on the physiochemical properties of the aqueous electrolytes [22, 68, 69]. In this sections, functional additives, such as small organic molecules, polymers, and salts, in the aqueous ZIBs are critically reviewed.

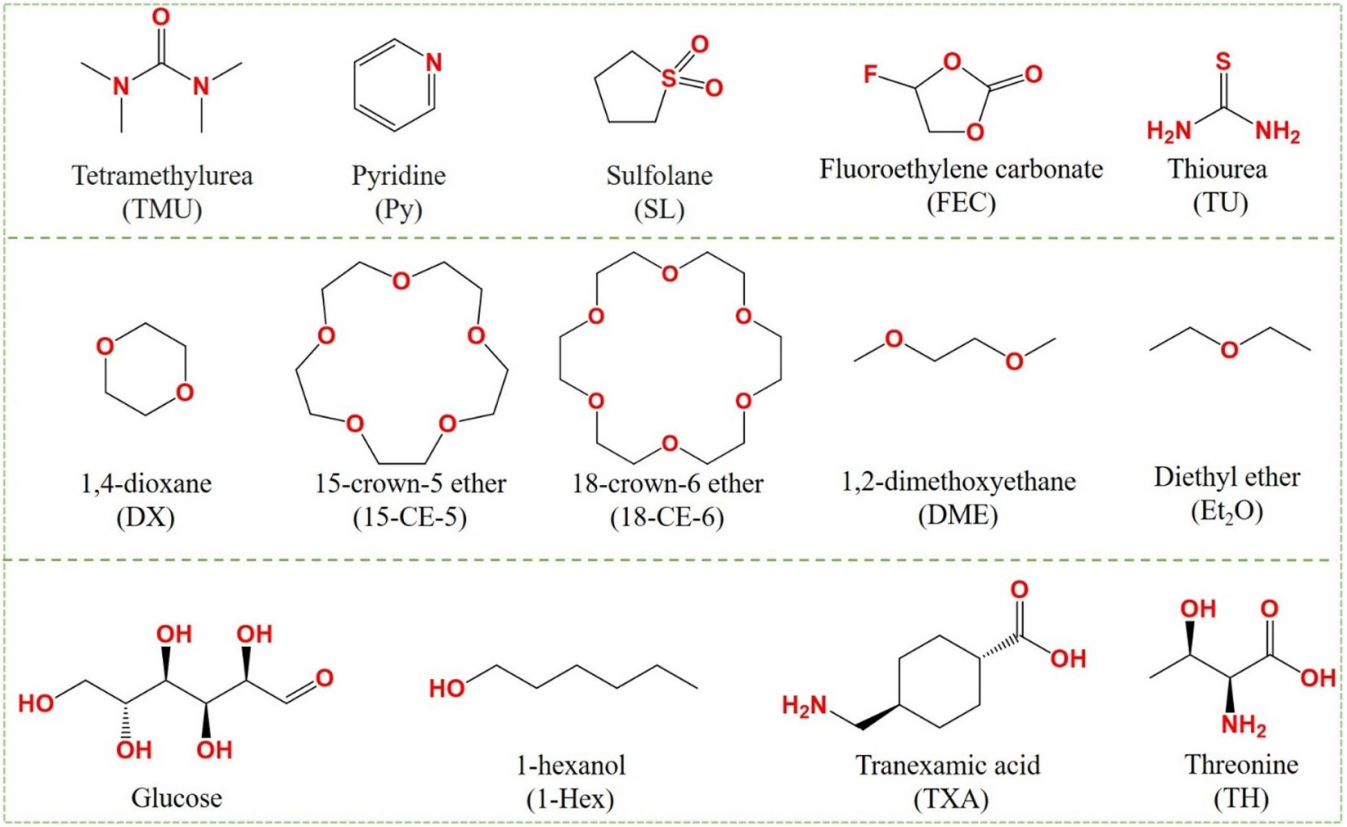

Figure 7. Molecular structures of typical organic small molecules used as functional additives in aqueous ZIBs.

4.1. Organic small molecules

Organic small molecules are used not only as co-solvents, but also as functional additives in aqueous electrolytes for ZIBs. Their working mechanisms include regulating Zn deposition by absorbing on the surface of Zn anode, breaking the original H-bonds and/or in situ construction of SEI by participation of solvation structures of Zn^{2+} [18, 65, 70–89]. In this section, we mainly focused on the manipulation of solvation structures by adoption of functional additives.

Similar with the organic small molecules used in co-solvents in 3.1 section, these organic small molecules possess polar functional groups (figure 7), in which the electron-rich atoms (O, N, S) interact with Zn^{2+}, alternating the solvation structures or de-solvation behavior of Zn^{2+}. For instance, Pyrinde (Py) has a high DN of 33, which is much higher than that of water (figure 8(a)), that is, the binding energy of Zn^{2+}-Py is much higher than that of Zn^{2+}-water (figure 8(b)), altering the solvation structure of Zn^{2+}. Moreover, due to the superior zincophilic of Py, inner Helmholtz plane (IHP) near the Zn anode is filled with Py-rich solvated complexes, as shown in figure 8(c), not only expelling water out of IHP, but also leading to homogenous deposition of Zn. The electrolytes with 1 vol.% Py enabled Zn||Cu cells with an average CE of 99.5%, Zn||Zn cells with cycling stability more than 3000 h at 0.5 mA cm^{-2}, Zn||$NaV_3O_8 \cdot 1.5H_2O$ (NVO) full cells with a capacity retention of 91.3% after 550 cycles [76]. Meng *et al* proposed a universal parameters, K, which represented the equilibrium constant of complexation reaction, to select appropriate additives. Ethylene diamine tetraacetic acid (EDTA), due to its high K (figure 8(e)), was selected as the functional additive in aqueous electrolytes. Due to the high binding energy of EDTA-Zn, EDTA entered into the primary solvation sheath of Zn^{2+}, and preferentially absorbed on the surface of Zn anode, effectively preventing the water-involved interfacial side reaction. Moreover, the energy barrier of the corrosion process in EDTA-involved electrolyte is higher than those in electrolytes with other additives, demonstrating its strong ability to inhibit the Zn corrosion. The aqueous electrolyte with addition of 0.05 M EDTA enabled Zn||Zn cells cycled for 3000 h at a high current density of 5 mA cm^{-2} [73].

Fluoroethylene carbonate (FEC) was also explored as functional additives in aqueous ZIBs. NMR spectra demonstrated that FEC changed the solvation structures of Zn^{2+} by replacing some water molecules with FEC, increasing the ratio of strong H-bonds while reducing that of weak H–bonds, thus resulting into suppression of water-involved side reactions (figure 8(f)). Moreover, FEC easily reacted with water in the aqueous electrolyte, producing HF, which further reacted with the byproducts on the surface of Zn, leading to compact Zn deposition. The aqueous electrolyte with 1 vol. % FEC highly improved the CE of Zn||Ti cells without obvious Zn dendrites [78]. Wei *et al* found that sulfolane (SL) could participated into the primary solvation structures due to the strong ESP of SL (figure 8(g)), leading to the higher ratio of (CIPs,

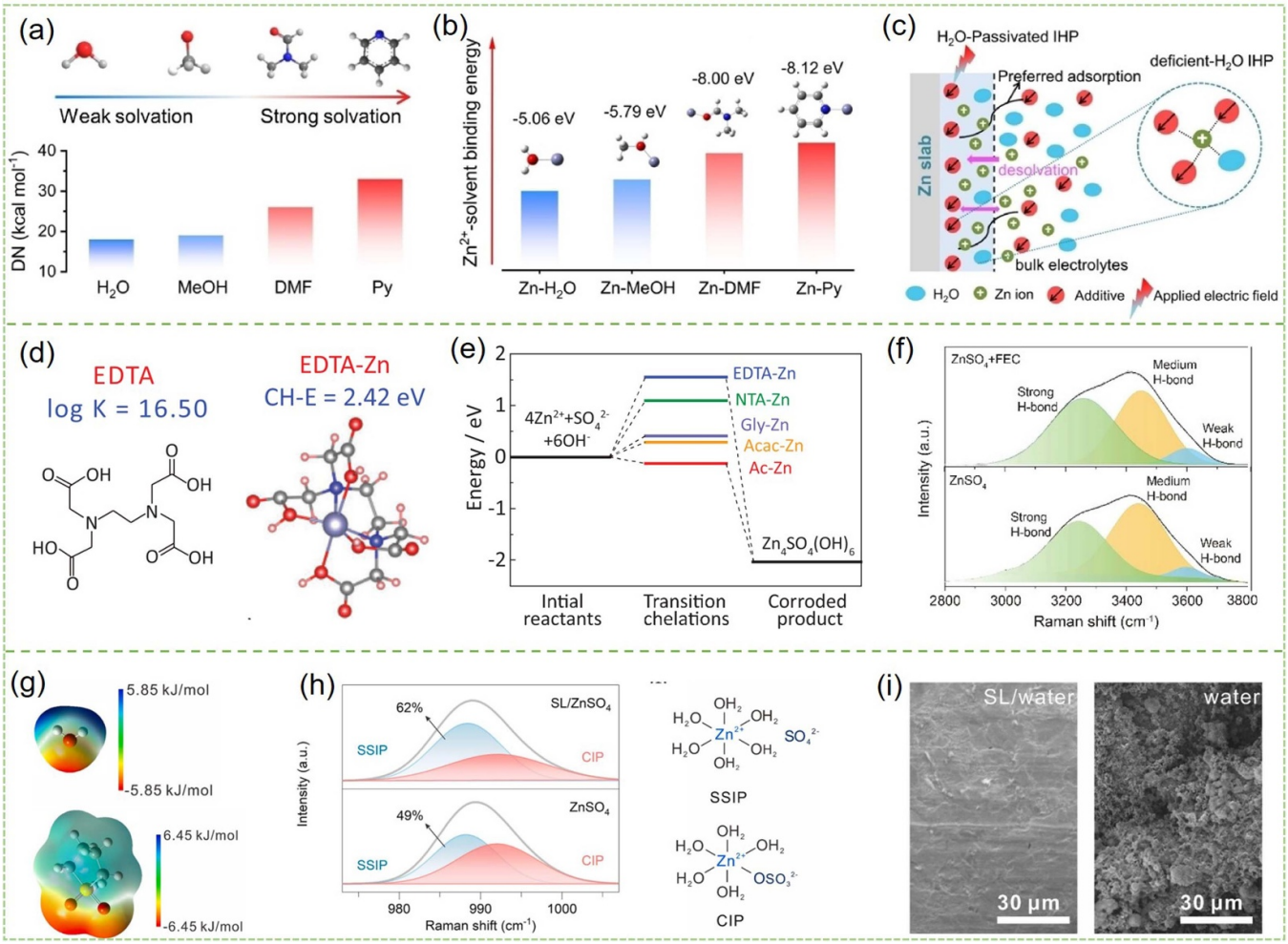

Figure 8. (a) DN of different small molecules. (b) Calculated binding energy between different complexes. (c) Molecular structures of typical organic small molecules used as functional additives in aqueous ZIBs [76]. John Wiley & Sons. [© 2023 Wiley-VCH GmbH]. (d) *k* value of EDTA, the binding energy of EDTA-Zn and the optimized molecular structures. (e) Energy barrier of interfacial corrosion in different electrolytes [73]. John Wiley & Sons. [© 2022 Wiley-VCH GmbH]. (f) Raman spectra of different electrolytes [78]. John Wiley & Sons. [© 2022 Wiley-VCH GmbH]. (g) ESP of different molecules, (h) Raman spectra of electrolytes with or without SL, (i) SEM images of Zn cycled in different electrolytes. Reprinted from [79], Copyright (2023), with permission from Elsevier.

figure 8(h)), both of which resulted into compact and dendrite-free Zn deposition, as shown in figure 8(i). The electrolytes with 11 vol. % SL not only enabled stable cycling of Zn||Cu and Zn||Zn cells, but also endowed Zn||V_2O_5 cells with a high capacity retention of 87.1% after 5000 cycles [79]. Besides, other organic small molecules such as 1,4-dioxane (DX) [70], vanillin [71] urea, LiOAC [72], thiourea (TU) [75, 85], glucose [77], 15-crown-5 ether (15-CE-5) [80], phytic acid (PA) [82], hexaoxacyclooctadecane (18C6) [83], tranexamic acid (TXA) [84], threonine (TH) [87], diethyl ether (Et_2O) [88], acetone [90], and etc. have been investigated, and their effect on the performance of ZIBs have been summarized in table 1.

4.2. Polymer additives

Polymers such as polyethylene oxide (PEO) [91, 92], polyacrylamide (PAM), and poly(sodium 4-styrenesulfonate) (PSS) [29], silk fibroin (SF) [93], silk peptide [94], and etc. have been widely investigated as functional additives in aqueous electrolytes for high-performance ZIBs. Yan *et al* systematically investigated different polymers such as PEO, PAM, and poly(sodium 4-styrenesulfonate) (PSS) as the functional additives in aqueous ZIBs. Compared with other polymers, Electrolytes PAM shown the best performance. Experimental and theoretical results both demonstrated that the addition of PAM additives could alter the solvation structures and double electrical layers near Zn anode, as shown in figures 9(a)–(c). Due to the polarity of PAM, it interacted with Zn^{2+} and water, appeared in the primary solvation sheath. Meanwhile, PAM is prone to be absorbed on the surface of Zn, altering the double electric layers near the anode, alleviating the side reactions and Zn deposition. As a result, 1 M ZnSO4 aqueous electrolyte with only 0.2 wt% highly improved the CE of Zn||Cu cells (99.65% over 1300 cycles) [29].

Biocompatible polymers such as SF and silk peptide were also used in aqueous electrolyte. Xu *et al* adopted 0.5 wt % SF as the additives, and it was found that the addition of SF changed the original solvation structures, leading to a SF

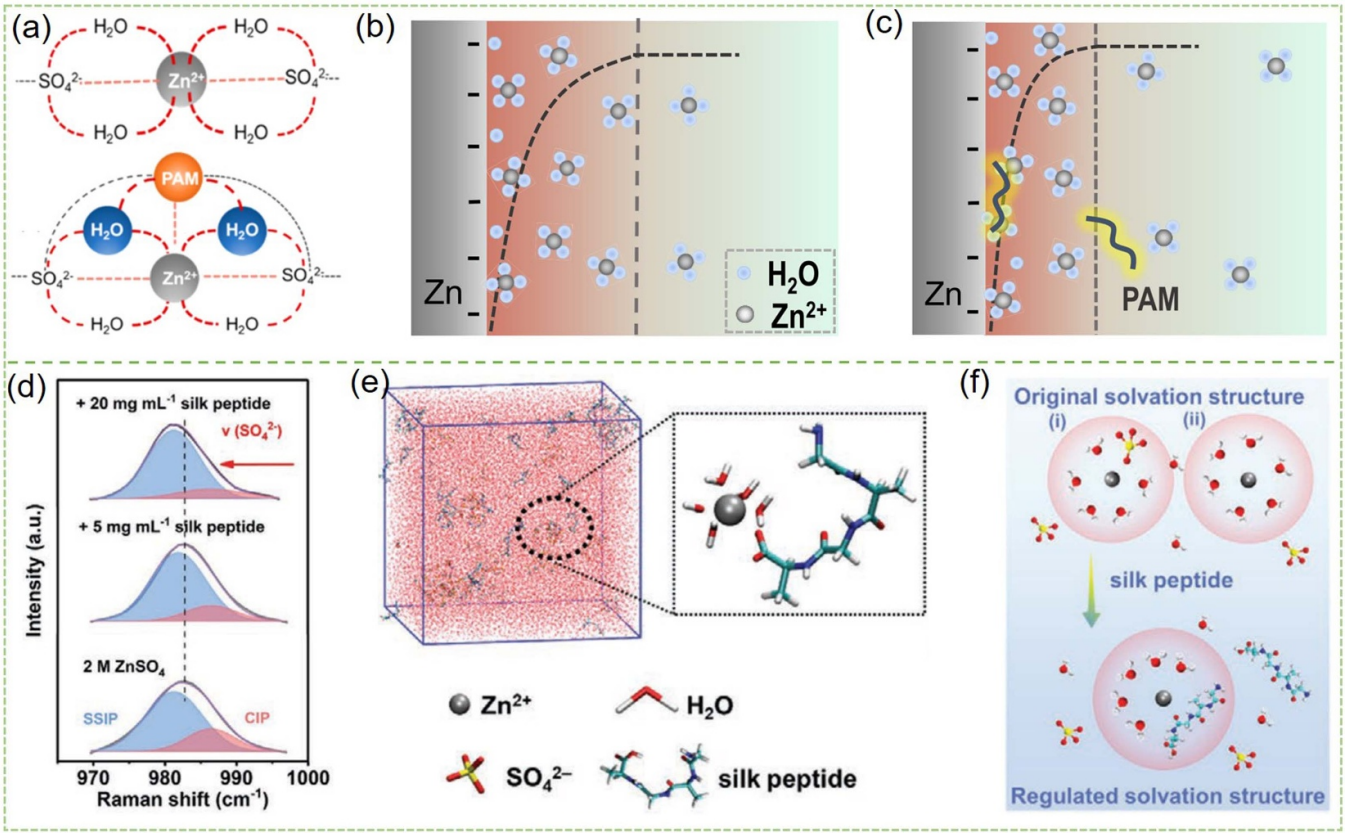

Figure 9. (a) Schematics of the bond network in different electrolytes, and schematical illustration of the double electrical layers near Zn anode (b) without and (c) with PMA. Reprinted with permission from [29]. Copyright (2021) American Chemical Society. (d) Raman spectra of electrolytes with or without silk peptide. (e) Snapshot of MD of aqueous electrolyte with silk peptide. (f) Schematics of solvation structures before and after addition of silk peptide [94]. John Wiley & Sons. [© 2022 Wiley-VCH GmbH].

protective film on the surface of anode, suppressing the formation of dendrites [93]. As shown in figure 9(d), the addition of silk peptide entered into the primary solvation structures of Zn^{2+}, which further expelled anions and water from solvation structure, reducing the ratio of CIPs in the solvation structures, which was also confirmed by MD simulation. The evolution of solvation structures with the addition of silk peptide were shown in figure 9(e). Consequently, an average of 99.7% after 1000 cycles was achieved in Cu||Zn cells, and a capacity retention of 76% after 1000 cycles was obtained in Zn-MnO2 full cells.

4.3. Salt additives

Inorganic salts, such as $MnSO_4$ and $CoSO_4$ are widely used as additives in ZIBs to suppress the transition metal dissolution from cathodes during the discharge-charge processes. Besides the additives to enhance the electrochemical performance of cathodes, salt additives including inorganic salts, ionic liquids, surfactant-type salts play key roles in anode stability [89, 95–102].

Bayaguud *et al* firstly explored the cationic surfactant-type salt, tetrabutylammonium sulfate (TBA_2SO_4) as the functional additives in aqueous electrolyte. The TBA^+ induced uniform and compact deposition of Zn via unique repulsion mechanism. As a result, with only 0.05 mM TBA_2SO_4, the designed electrolytes enabled Zn||Zn symmetric cells stable cycling of 400 h even at a high current density of 10 mA cm^{-2}.

Lv *et al* investigated the effect of ionic liquids on the solvation structures and the corresponding electrochemical performances. Four different zwitterionic ionic liquids were investigated in this work, and it was found that a unique self-adaptive electric double layer (EDL) was successfully constructed on the surface of both anode and cathode with 3-(1-methylimidazole) propanesulfonate (ImS) as the additive. MD results demonstrated that one of the water molecules in the original solvation structure was replaced by one ImS, moreover, the cationic part of ImS was adsorbed on surface of the negatively charged Zn metal and the anionic part interacted tightly with Zn^{2+}. The unique EDL not only inhibited the structural instability of cathode, but also led to uniform deposition of Zn, thus resulting in significantly improved electrochemical performances of Zn||Cu, Zn||Zn symmetric cells, and Zn||NVOH full cells.

Beside, inorganic salts were also investigated in aqueous ZIBs [98]. For instance, Scandium triflate was introduced into aqueous electrolytes for ZIBs, leading to formation of rigid solvation shell around Sc^{3+}, with its tip-blocking effect, further resulting into uniform Zn deposition. Therefore, Zn||Cu cells with a CE of 99.5% over 100 cycles at a current density of 4 mA cm^{-2}, and full cells maintaining their capacity after

more than 5000 cycles were successfully constructed with the additive of Sc^{3+} [100].

5. Conclusion

In this review, we mainly summarized the development of zinc salts, nonaqueous solvents, and functional additives in aqueous electrolyte, and their effects on the solvation structures of Zn^{2+} and the corresponding electrochemical performances of ZIBs. In general, the strategies of regulating Zn^{2+} solvation structures by introducing different zinc salts, nonaqueous solvents and functional additives, and their working mechanism in taming Zn deposition, suppressing H_2 evolution, and inhabiting Zn corrosions have been critically summarized. Specifically, the type and concentration of zinc salts, organic solvents (ethers, esters, alcohols, and etc.) and polymers as the co-solvent, various functional additives (organic small molecules, polymers, and salts) have been thoroughly reviewed, all of which could significantly alter the solvation structures of Zn^{2+}, further reducing the active water and/or leading to robust SEI, suppressing the Zn dendrite and interfacial side reactions. This review not only provides the recent development of aqueous electrolytes in ZIBs, but also is enlightening for further design of high-performance electrolytes for aqueous ZIBs.

6. Future perspectives

Although great progresses have been made in aqueous ZIBs, their commercial application is still plagued by their low energy density, inferior cycling stability, and industrial feasibility. For instance, compared with Zn foil, Zn power, due to its low cost and processability, is more suitable for industrial application. However, Zn power suffered from severer dendrites and the interfacial side reactions; the change of the solvation structures of Zn^{2+} not only manipulated the SEI and decreased the free water, but also alleviated the 'tip effect' of deposited Zn, but the effect of solvation structure on the cathode-electrolyte interphases, the stability of cathodes, and the electrochemical kinetics are not clearly illustrated. In addition, broadening the ESPWs is an effective way to improve the energy density, which is highly challenging in aqueous electrolytes. Moreover, understanding the structure-property relationships and the fundamental electrochemical mechanism are indispensable for designing novel electrolytes and constructing high-performance aqueous ZIBs. To overcoming the above challenges, the following issues or strategies need to be addressed or adopted (figure 10):

(1) Structure-properties relationships in aqueous electrolytes. Although abundant strategies have been summarized in this review, the research on novel electrolytes are mainly based on 'trial and error' paradigm, how to design electrolytes according to the requirement is still highly challenging. Understanding the structure-properties relationship in the aqueous electrolytes is the prerequisite. For instance, how the molecular structures of components in the aqueous electrolyte affect the solvation structures of Zn^{2+}, what is the influence of solvation structures on the structure or component of SEI, desolvation energy of Zn^{2+}, Zn deposition behavior, and the ESPWs, and what is the relationship between structure and component of SEI and Zn deposition behavior, ESPWs, and Zn corrosion process, all of which is significantly important to design high-performance aqueous electrolytes. Therefore, figuring out the structure-properties relationships is the prerequisite to effectively design novel aqueous electrolytes.

(2) Practical consideration of the massive application. Firstly, most of the researches only focused on the effect of electrolyte on the performance of half cells, only a few studies take the weight ratio of electrolytes in the full cells into consideration. Using flooded electrolytes is beneficial for cycling stability, which, however, decreases the energy density. Therefore, lean electrolyte should take into consideration when evaluating its commercial feasibility. Secondly, cost is another factor affecting the commercial application of electrolytes. Take HCEs for example, although increasing the concentration of zinc salts highly improve the electrochemical performance, the dramatical cost increase hinder their future application. Thirdly, compatibility with other components of ZIBs (such as current collectors and separators) and environment benign [103–106]. Thus, in our opinion, aqueous electrolyte with functional additives or organic co-solvents, compared with HCEs, are more promising for commercial application.

(3) Advanced techniques. Exploring the multiscale relationship of 'molecular structure-solvation structure-SEI-electrochemical performance of pouch cells' (from subnanometer to meters) is very challenging [107–110]. Meanwhile, the electrochemical process is dynamic process under confined spaces, making *in-situ* or *operando* characterization much challenging. Thus, adopting advanced *in-situ* or *operando* characterizations is pivotal to illustrate the fundamental mechanism [111, 112]. Advance techniques such as *in-situ* transmission electron miscopy, atomic force microscope, cryo-electron microscopy, electrochemical quartz crystal microbalance, scanning electrochemical microscopy, differential electrochemical mass spectroscopy, and *operando* Fourier transform infrared spectroscopy, Raman spectroscopy, NMR, x-ray computed tomography are necessary, which should be used individually or with each other [113–118].

(4) Data-driven discovery of novel electrolytes. Discovery of novel materials based on traditional 'trials and errors' is expensive and time-consuming. The emerging data-drive model (including artificial intelligence or machine learning) have been widely adopted in the discovery of novel functional materials, which open avenues for designing novel aqueous electrolyte [119, 120]. Based on the massive data, various machine learning models (such as deep neutral networks, decision trees, and etc.) could be trained and further used to

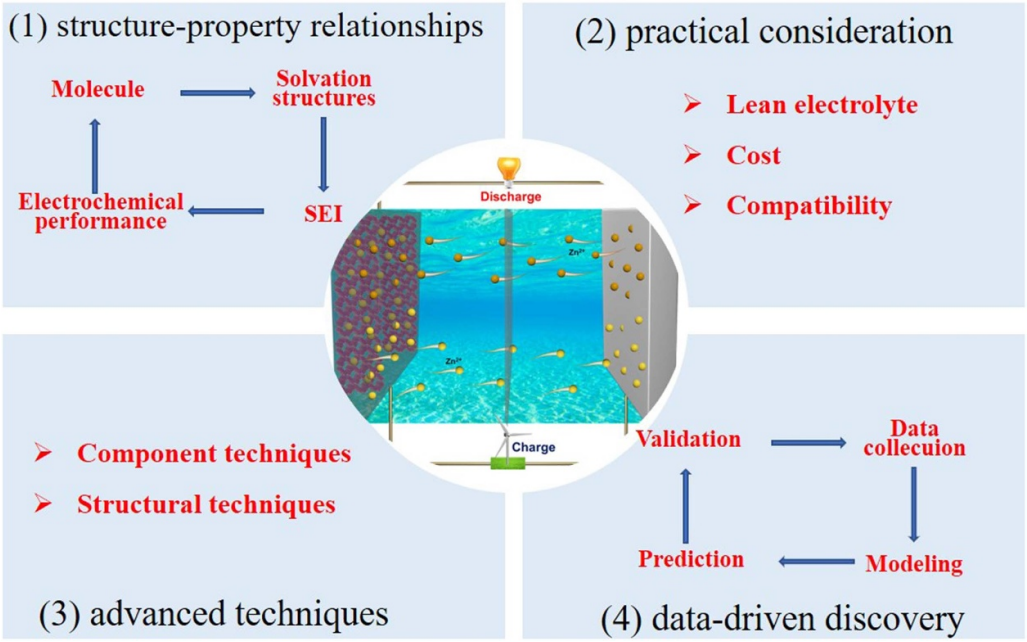

Figure 10. The challenges and possible strategies for the future application of aqueous ZIBs.

design ideal molecules for aqueous electrolytes, in which the massive data are collected from experiments, theoretical calculation, databases or references. Machine learning models are not only constructed to design of novel molecules, but also trained to synthesize materials and predict their properties [121–127]. Based on the data-drive paradigm, accelerating the discovery of novel materials of high-performance aqueous ZIBs with low cost is highly promising.

Acknowledgments

This work was supported by Natural Science Foundation of Hunan Province (2023JJ40662), National Defense Science and Technology Key Laboratory Supporting Project (WDZC20235250508), National Natural Science Foundation (22002186), Seed Fund of National University of Defense Technology.

Conflict of interest

There are no conflicts to declare.

Author's contribution

P Xiao conducted Project administration, writing-original draft, writing-review & editing, funding acquisition, and conceptualization. W Zhang conducted writing-original draft. Y Chen and C Zheng conducted supervision. H Gao, P Gao, and W Xie conducted validation and writing-review & editing.

ORCID iD

Peitao Xiao https://orcid.org/0000-0002-4262-2444

References

[1] Xu K 2004 Nonaqueous liquid electrolytes for lithium-based rechargeable batteries *Chem. Rev.* **104** 4303–418
[2] Xu K 2014 Electrolytes and interphases in Li-ion batteries and beyond *Chem. Rev.* **114** 11503–618
[3] Xiao P, Yun X, Chen Y, Guo X, Gao P, Zhou G and Zheng C 2023 Insights into the solvation chemistry in liquid electrolytes for lithium-based rechargeable batteries *Chem. Soc. Rev.* (https://doi.org/10.1039/D3CS00151B)
[4] Blanc L E, Kundu D and Nazar L F 2020 Scientific challenges for the implementation of Zn-ion batteries *Joule* **4** 771–99
[5] Liu S, Zhang R, Mao J, Zhao Y, Cai Q and Guo Z 2022 From room temperature to harsh temperature applications: fundamentals and perspectives on electrolytes in zinc metal batteries *Sci. Adv.* **8** eabn5097
[6] Zhong X *et al* 2023 Flexible zinc-air batteries with ampere-hour capacities and wide-temperature adaptabilities *Adv. Mater.* **35** 2209980
[7] Huang Q, Zhong X, Zhang Q, Wu X, Jiao M, Chen B, Sheng J and Zhou G 2022 Co_3O_4/Mn_3O_4 hybrid catalysts with heterointerfaces as bifunctional catalysts for Zn-air batteries *J. Energy Chem.* **68** 679–87
[8] Zhou L, Wang F, Yang F, Liu X, Yu Y, Zheng D and Lu X 2022 Unshared pair electrons of zincophilic lewis base enable long-life Zn anodes under "three high" conditions *Angew. Chem., Int. Ed.* **61** 202208051
[9] Jiao M, Zhang Q, Ye C, Zhong X, Wang J, Li C, Dai L, Zhou G and Cheng H M 2022 Recycling spent $LiNi_{1-x-y}Mn_xCo_yO_2$ cathodes to bifunctional NiMnCo catalysts for zinc-air batteries *Proc. Natl Acad. Sci. USA* **119** e2202202119

[10] Yun X, Chen Y, Xiao P and Zheng C 2022 Review on oxygen-free vanadium-based cathodes for aqueous zinc-ion batteries *J. Electrochem.* **28** 2219004

[11] Qiu H, Du X, Zhao J, Wang Y, Ju J, Chen Z, Hu Z, Yan D, Zhou X and Cui G 2019 Zinc anode-compatible in-situ solid electrolyte interphase via cation solvation modulation *Nat. Commun.* **10** 5374

[12] Zhong C *et al* 2020 Decoupling electrolytes towards stable and high-energy rechargeable aqueous zinc–manganese dioxide batteries *Nat. Energy* **5** 440–9

[13] Xiao P, Luo R, Piao Z, Li C, Wang J, Yu K, Zhou G and Cheng H-M 2021 High-performance lithium metal batteries with a wide operating temperature range in carbonate electrolyte by manipulating interfacial chemistry *ACS Energy Lett.* **6** 3170–9

[14] Chen Y *et al* 2022 Engineering an insoluble cathode electrolyte interphase enabling high performance NCM811//graphite pouch cell at 60 °C *Adv. Energy Mater.* **12** 2201631

[15] Li Z, Chen Y, Yun X, Gao P, Zheng C and Xiao P 2023 Critical review of fluorinated electrolytes for high-performance lithium metal batteries *Adv. Funct. Mater.* 2300502

[16] Lv Y, Xiao Y, Ma L, Zhi C and Chen S 2022 Recent advances in electrolytes for "beyond aqueous" zinc-ion batteries *Adv. Mater.* **34** 2106409

[17] Li X, Wang X, Ma L and Huang W 2022 Solvation structures in aqueous metal-ion batteries *Adv. Energy Mater.* **12** 2202068

[18] Wang D, Li Q, Zhao Y, Hong H, Li H, Huang Z, Liang G, Yang Q and Zhi C 2022 Insight on organic molecules in aqueous Zn-ion batteries with an emphasis on the Zn anode regulation *Adv. Energy Mater.* **12** 2102707

[19] Wu K, Huang J, Yi J, Liu X, Liu Y, Wang Y, Zhang J and Xia Y 2020 Recent advances in polymer electrolytes for zinc ion batteries: mechanisms, properties, and perspectives *Adv. Energy Mater.* **10** 1903977

[20] Cao J, Zhang D, Zhang X, Zeng Z, Qin J and Huang Y 2022 Strategies of regulating Zn^{2+} solvation structures for dendrite-free and side reaction-suppressed zinc-ion batteries *Energy Environ. Sci.* **15** 499–528

[21] Zhang L, Rodríguez-Pérez I A, Jiang H, Zhang C, Leonard D P, Guo Q, Wang W, Han S, Wang L and Ji X 2019 $ZnCl_2$ "water-in-salt" electrolyte transforms the performance of vanadium oxide as a Zn battery cathode *Adv. Funct. Mater.* **29** 1902653

[22] Du Y, Li Y, Xu B B, Liu T X, Liu X, Ma F, Gu X and Lai C 2022 Electrolyte salts and additives regulation enables high performance aqueous zinc ion batteries: a mini review *Small* **18** e2104640

[23] Zhang N, Cheng F, Liu Y, Zhao Q, Lei K, Chen C, Liu X and Chen J 2016 Cation-deficient spinel $ZnMn_2O_4$ cathode in $Zn(CF_3SO_3)_2$ electrolyte for rechargeable aqueous Zn-ion battery *J. Am. Chem. Soc.* **138** 12894–901

[24] Peng Z, Wei Q, Tan S, He P, Luo W, An Q and Mai L 2018 Novel layered iron vanadate cathode for high-capacity aqueous rechargeable zinc batteries *Chem. Commun.* **54** 4041–4

[25] Wang L, Zhang Y, Hu H, Shi H Y, Song Y, Guo D, Liu X X and Sun X 2019 A $Zn(ClO_4)_2$ electrolyte enabling long-life zinc metal electrodes for rechargeable aqueous zinc batteries *ACS Appl. Mater. Interfaces* **11** 42000–5

[26] Zhu Y, Yin J, Zheng X, Emwas A-H, Lei Y, Mohammed O F, Cui Y and Alshareef H N 2021 Concentrated dual-cation electrolyte strategy for aqueous zinc-ion batteries *Energy Environ. Sci.* **14** 4463–73

[27] Wang J, Yang Y, Wang Y, Dong S, Cheng L, Li Y, Wang Z, Trabzon L and Wang H 2022 Working aqueous Zn metal batteries at 100 degrees C *ACS Nano* **16** 15770–8

[28] Qin R *et al* 2021 Tuning Zn^{2+} coordination environment to suppress dendrite formation for high-performance Zn-ion batteries *Nano Energy* **80** 105478

[29] Yan M, Dong N, Zhao X, Sun Y and Pan H 2021 Tailoring the stability and kinetics of Zn anodes through trace organic polymer additives in dilute aqueous electrolyte *ACS Energy Lett.* **6** 3236–43

[30] Geng L *et al* 2022 Eutectic electrolyte with unique solvation structure for high-performance zinc-ion batteries *Angew. Chem., Int. Ed.* **61** e202206717

[31] Tang X, Wang P, Bai M, Wang Z, Wang H, Zhang M and Ma Y 2021 Unveiling the reversibility and stability origin of the aqueous V_2 O_5 -Zn batteries with a $ZnCl_2$ "water-in-salt" electrolyte *Adv. Sci.* **8** e2102053

[32] Wang F, Borodin O, Gao T, Fan X, Sun W, Han F, Faraone A, Dura J A, Xu K and Wang C 2018 Highly reversible zinc metal anode for aqueous batteries *Nat. Mater.* **17** 543–9

[33] Wan F, Zhang Y, Zhang L, Liu D, Wang C, Song L, Niu Z and Chen J 2019 Reversible oxygen redox chemistry in aqueous zinc-ion batteries *Angew. Chem., Int. Ed.* **58** 7062–7

[34] Li C, Yuan W, Li C, Wang H, Wang L, Liu Y and Zhang N 2021 Boosting Li_3V_2 $(PO_4)_3$ cathode stability using a concentrated aqueous electrolyte for high-voltage zinc batteries *Chem. Commun.* **57** 4319–22

[35] Zhao J, Zhang J, Yang W, Chen B, Zhao Z, Qiu H, Dong S, Zhou X, Cui G and Chen L 2019 "Water-in-deep eutectic solvent" electrolytes enable zinc metal anodes for rechargeable aqueous batteries *Nano Energy* **57** 625–34

[36] Lin X, Zhou G, Robson M J, Yu J, Kwok S C T and Ciucci F 2021 Hydrated deep eutectic electrolytes for high-performance Zn-ion batteries capable of low-temperature operation *Adv. Funct. Mater.* **32** 2109322

[37] Yang M, Zhu J, Bi S, Wang R and Niu Z 2022 A binary hydrate-melt electrolyte with acetate-oriented cross-linking solvation shells for stable zinc anodes *Adv. Mater.* **34** e2201744

[38] Ma L *et al* 2021 Functionalized phosphonium cations enable zinc metal reversibility in aqueous electrolytes *Angew. Chem., Int. Ed.* **60** 12438–45

[39] Yang H, Chang Z, Qiao Y, Deng H, Mu X, He P and Zhou H 2020 Constructing a super-saturated electrolyte front surface for stable rechargeable aqueous zinc batteries *Angew. Chem., Int. Ed.* **59** 9377–81

[40] Yang H, Qiao Y, Chang Z, Deng H, Zhu X, Zhu R, Xiong Z, He P and Zhou H 2021 Reducing water activity by zeolite molecular sieve membrane for long-life rechargeable zinc battery *Adv. Mater.* **33** e2102415

[41] Zhang Q, Ma Y, Lu Y, Li L, Wan F, Zhang K and Chen J 2020 Modulating electrolyte structure for ultralow temperature aqueous zinc batteries *Nat. Commun.* **11** 4463

[42] Sun T, Yuan X, Wang K, Zheng S, Shi J, Zhang Q, Cai W, Liang J and Tao Z 2021 An ultralow-temperature aqueous zinc-ion battery *J. Mater. Chem.* A **9** 7042–7

[43] Wang R, Yao M, Yang M, Zhu J, Chen J and Niu Z 2023 Synergetic modulation on ionic association and solvation structure by electron-withdrawing effect for aqueous zinc-ion batteries *Proc. Natl Acad. Sci. USA* **120** e2221980120

[44] Kundu D, Hosseini Vajargah S, Wan L, Adams B, Prendergast D and Nazar L F 2018 Aqueous vs. nonaqueous Zn-ion batteries: consequences of the desolvation penalty at the interface *Energy Environ. Sci.* **11** 881–92

[45] Segler M H S, Preuss M and Waller M P 2018 Planning chemical syntheses with deep neural networks and symbolic AI *Nature* **555** 604–10

[46] Yang W *et al* 2020 Hydrated eutectic electrolytes with ligand-oriented solvation shells for long-cycling zinc-organic batteries *Joule* **4** 1557–74

[47] Han D *et al* 2021 A non-flammable hydrous organic electrolyte for sustainable zinc batteries *Nat. Sustain.* **5** 205–13

[48] Ming F, Zhu Y, Huang G, Emwas A H, Liang H, Cui Y and Alshareef H N 2022 Co-solvent electrolyte engineering for stable anode-free zinc metal batteries *J. Am. Chem. Soc.* **144** 7160–70

[49] Liu S, Mao J, Pang W K, Vongsvivut J, Zeng X, Thomsen L, Wang Y, Liu J, Li D and Guo Z 2021 Tuning the electrolyte solvation structure to suppress cathode dissolution, water reactivity, and Zn dendrite growth in zinc-ion batteries *Adv. Funct. Mater.* **31** 2104281

[50] Miao L *et al* 2022 Aqueous electrolytes with hydrophobic organic cosolvents for stabilizing zinc metal anodes *ACS Nano* **16** 9667–78

[51] Liu D S *et al* 2022 Regulating the electrolyte solvation structure enables ultralong lifespan vanadium-based cathodes with excellent low-temperature performance *Adv. Funct. Mater.* **32** 2111714

[52] Qiu B, Xie L, Zhang G, Cheng K, Lin Z, Liu W, He C, Zhang P and Mi H 2022 Toward reversible wide-temperature Zn storage by regulating the electrolyte solvation structure via trimethyl phosphate *Chem. Eng. J.* **449** 137843

[53] Dong Y, Miao L, Ma G, Di S, Wang Y, Wang L, Xu J and Zhang N 2021 Non-concentrated aqueous electrolytes with organic solvent additives for stable zinc batteries *Chem. Sci.* **12** 5843–52

[54] Ma G, Miao L, Dong Y, Yuan W, Nie X, Di S, Wang Y, Wang L and Zhang N 2022 Reshaping the electrolyte structure and interface chemistry for stable aqueous zinc batteries *Energy Storage Mater.* **47** 203–10

[55] Hao J, Yuan L, Ye C, Chao D, Davey K, Guo Z and Qiao S Z 2021 Boosting zinc electrode reversibility in aqueous electrolytes by using low-cost antisolvents *Angew. Chem., Int. Ed.* **60** 7366–75

[56] Cao L, Li D, Hu E, Xu J, Deng T, Ma L, Wang Y, Yang X Q and Wang C 2020 Solvation structure design for aqueous Zn metal batteries *J. Am. Chem. Soc.* **142** 21404–9

[57] Li T C, Lim Y, Li X L, Luo S, Lin C, Fang D, Xia S, Wang Y and Yang H Y 2022 A universal additive strategy to reshape electrolyte solvation structure toward reversible Zn storage *Adv. Energy Mater.* **12** 2103231

[58] Du H, Wang K, Sun T, Shi J, Zhou X, Cai W and Tao Z 2022 Improving zinc anode reversibility by hydrogen bond in hybrid aqueous electrolyte *Chem. Eng. J.* **427** 131705

[59] Li C, Kingsbury R, Zhou L, Shyamsunder A, Persson K A and Nazar L F 2022 Tuning the solvation structure in aqueous zinc batteries to maximize Zn-ion intercalation and optimize dendrite-free zinc plating *ACS Energy Lett.* **7** 533–40

[60] Wu Y, Zhu Z, Shen D, Chen L, Song T, Kang T, Tong Z, Tang Y, Wang H and Lee C S 2022 Electrolyte engineering enables stable Zn-Ion deposition for long-cycling life aqueous Zn-ion batteries *Energy Storage Mater.* **45** 1084–91

[61] Sun Y *et al* 2022 Low-cost and long-life Zn/Prussian blue battery using a water-in-ethanol electrolyte with a normal salt concentration *Energy Storage Mater.* **48** 192–204

[62] Zhang Y, Zhu M, Wu K, Yu F, Wang G, Xu G, Wu M, Liu H-K, Dou S-X and Wu C 2021 An in-depth insight of a highly reversible and dendrite-free Zn metal anode in an hybrid electrolyte *J. Mater. Chem.* A **9** 4253–61

[63] Chang N, Li T, Li R, Wang S, Yin Y, Zhang H and Li X 2020 An aqueous hybrid electrolyte for low-temperature zinc-based energy storage devices *Energy Environ. Sci.* **13** 3527–35

[64] Yang J *et al* 2022 Three birds with one stone: tetramethylurea as electrolyte additive for highly reversible Zn-metal anode *Adv. Funct. Mater.* **32** 2209642

[65] Li Z, Liao Y, Wang Y, Cong J, Ji H, Huang Z and Huang Y 2023 A co-solvent in aqueous electrolyte towards ultralong-life rechargeable zinc-ion batteries *Energy Storage Mater.* **56** 174–82

[66] Deng W, Xu Z and Wang X 2022 High-donor electrolyte additive enabling stable aqueous zinc-ion batteries *Energy Storage Mater.* **52** 52–60

[67] Wu F, Chen Y, Chen Y, Yin R, Feng Y, Zheng D, Xu X, Shi W, Liu W and Cao X 2022 Achieving highly reversible zinc anodes via N, N-dimethylacetamide enabled Zn-ion solvation regulation *Small* **18** e2202363

[68] Ma L *et al* 2018 Initiating a mild aqueous electrolyte Co_3O_4/Zn battery with 2.2 V-high voltage and 5000-cycle lifespan by a Co(iii) rich-electrode *Energy Environ. Sci.* **11** 2521–30

[69] Pan H *et al* 2016 Reversible aqueous zinc/manganese oxide energy storage from conversion reactions *Nat. Energy* **1** 16039

[70] Feng R, Chi X, Qiu Q, Wu J, Huang J, Liu J and Liu Y 2021 Cyclic ether-water hybrid electrolyte-guided dendrite-free lamellar zinc deposition by tuning the solvation structure for high-performance aqueous zinc-ion batteries *ACS Appl. Mater. Interfaces* **13** 40638–47

[71] Zhao K, Liu F, Fan G, Liu J, Yu M, Yan Z, Zhang N and Cheng F 2021 Stabilizing zinc electrodes with a vanillin additive in mild aqueous electrolytes *ACS Appl. Mater. Interfaces* **13** 47650–8

[72] Feng X, Li P, Yin J, Gan Z, Gao Y, Li M, Cheng Y, Xu X, Su Y and Ding S 2023 Enabling highly reversible Zn anode by multifunctional synergistic effects of hybrid solute additives *ACS Energy Lett.* **8** 1192–200

[73] Meng R, Li H, Lu Z, Zhang C, Wang Z, Liu Y, Wang W, Ling G, Kang F and Yang Q H 2022 Tuning Zn-ion solvation chemistry with chelating ligands toward stable aqueous Zn anodes *Adv. Mater.* **34** e2200677

[74] Zhang H, Zhong Y, Li J, Liao Y, Zeng J, Shen Y, Yuan L, Li Z and Huang Y 2022 Inducing the preferential growth of Zn (002) plane for long cycle aqueous Zn-ion batteries *Adv. Energy Mater.* **13** 2203254

[75] Qin H, Kuang W, Hu N, Zhong X, Huang D, Shen F, Wei Z, Huang Y, Xu J and He H 2022 Building metal-molecule interface towards stable and reversible Zn metal anodes for aqueous rechargeable zinc batteries *Adv. Funct. Mater.* **32** 2206695

[76] Luo J *et al* 2023 Regulating the inner helmholtz plane with a high donor additive for efficient anode reversibility in aqueous Zn-ion batteries *Angew. Chem., Int. Ed.* **62** e202302302

[77] Sun P, Ma L, Zhou W, Qiu M, Wang Z, Chao D and Mai W 2021 Simultaneous regulation on solvation shell and electrode interface for dendrite-free Zn ion batteries achieved by a low-cost glucose additive *Angew. Chem., Int. Ed.* **60** 18247–55

[78] Xie D, Sang Y, Wang D H, Diao W Y, Tao F Y, Liu C, Wang J W, Sun H Z, Zhang J P and Wu X L 2023 ZnF_2 -riched inorganic/organic hybrid SEI: in situ-chemical construction and performance-improving mechanism for aqueous zinc-ion batteries *Angew. Chem., Int. Ed.* **62** e202216934

[79] Wei T, Zhang X, Ren Y, Wang Y, Li Z, Zhang H and Hu L 2023 Reconstructing anode/electrolyte interface and solvation structure towards high stable zinc anode *Chem. Eng. J.* **457** 141272

[80] Xin T, Zhou R, Xu Q, Yuan X, Zheng Z, Li Y, Zhang Q and Liu J 2023 15-Crown-5 ether as efficient electrolyte additive for performance enhancement of aqueous Zn-ion batteries *Chem. Eng. J.* **452** 139572

[81] Chen Y, Gong F, Deng W, Zhang H and Wang X 2023 Dual-function electrolyte additive enabling simultaneous electrode interface and coordination environment regulation for zinc-ion batteries *Energy Storage Mater.* **58** 20–29

[82] Hu Q, Hu J, Li L, Ran Q, Ji Y, Liu X, Zhao J and Xu B 2023 In-depth study on the regulation of electrode interface and solvation structure by hydroxyl chemistry *Energy Storage Mater.* **54** 374–81

[83] Li R, Li M, Chao Y, Guo J, Xu G, Li B, Liu Z and Yang C 2022 Hexaoxacyclooctadecane induced interfacial engineering to achieve dendrite-free Zn ion batteries *Energy Storage Mater.* **46** 605–12

[84] Yin J *et al* 2023 Integrated electrolyte regulation strategy: trace trifunctional tranexamic acid additive for highly reversible Zn metal anode and stable aqueous zinc ion battery *Energy Storage Mater.* **59** 102800

[85] Wu X *et al* 2015 The electrochemical performance improvement of $LiMn_2O_4$/Zn based on zinc foil as the current collector and thiourea as an electrolyte additive *J. Power Sources* **300** 453–9

[86] Cui J, Liu X, Xie Y, Wu K, Wang Y, Liu Y, Zhang J, Yi J and Xia Y 2020 Improved electrochemical reversibility of Zn plating/stripping: a promising approach to suppress water-induced issues through the formation of H-bonding *Mater. Today Energy* **18** 100563

[87] Miao Z *et al* 2022 Unveiling unique steric effect of threonine additive for highly reversible Zn anode *Nano Energy* **97** 107145

[88] Xu W, Zhao K, Huo W, Wang Y, Yao G, Gu X, Cheng H, Mai L, Hu C and Wang X 2019 Diethyl ether as self-healing electrolyte additive enabled long-life rechargeable aqueous zinc ion batteries *Nano Energy* **62** 275–81

[89] Wang M, Cheng Y, Zhao H, Gao J, Li J, Wang Y, Qiu J, Zhang H, Chen X and Wei Y 2023 A multifunctional organic electrolyte additive for aqueous zinc ion batteries based on polyaniline cathode *Small* **19** 2302105

[90] Shi X, Wang J, Yang F, Liu X, Yu Y and Lu X 2022 Metallic zinc anode working at 50 and 50 mAh cm^{-2} with high depth of discharge via electrical double layer reconstruction *Adv. Funct. Mater.* **33** 2211917

[91] Jin Y, Han K S, Shao Y, Sushko M L, Xiao J, Pan H and Liu J 2020 Stabilizing zinc anode reactions by polyethylene oxide polymer in mild aqueous electrolytes *Adv. Funct. Mater.* **30** 2003932

[92] Yan M, Xu C, Sun Y, Pan H and Li H 2021 Manipulating Zn anode reactions through salt anion involving hydrogen bonding network in aqueous electrolytes with PEO additive *Nano Energy* **82** 105739

[93] Xu J *et al* 2022 In situ construction of protective films on Zn metal anodes via natural protein additives enabling high-performance zinc ion batteries *ACS Nano* **16** 11392–404

[94] Wang B, Zheng R, Yang W, Han X, Hou C, Zhang Q, Li Y, Li K and Wang H 2022 Synergistic solvation and interface regulations of eco-friendly silk peptide additive enabling stable aqueous zinc-ion batteries *Adv. Funct. Mater.* **32** 2112693

[95] Bayaguud A, Luo X, Fu Y and Zhu C 2020 Cationic surfactant-type electrolyte additive enables three-dimensional dendrite-free zinc anode for stable zinc-ion batteries *ACS Energy Lett.* **5** 3012–20

[96] Wan J *et al* 2023 A double-functional additive containing nucleophilic groups for high-performance Zn-ion batteries *ACS Nano* **17** 1610–21

[97] Zeng X *et al* 2021 Electrolyte design for in situ construction of highly Zn^{2+} -conductive solid electrolyte interphase to enable high-performance aqueous Zn-ion batteries under practical conditions *Adv. Mater.* **33** e2007416

[98] Wang P, Xie X, Xing Z, Chen X, Fang G, Lu B, Zhou J, Liang S and Fan H J 2021 Mechanistic insights of Mg^{2+} -electrolyte additive for high-energy and long-life zinc-ion hybrid capacitors *Adv. Energy Mater.* **11** 2101158

[99] Cao L *et al* 2021 Highly reversible aqueous zinc batteries enabled by zincophilic-zincophobic interfacial layers and interrupted hydrogen-bond electrolytes *Angew. Chem., Int. Ed.* **60** 18845–51

[100] Kim M, Shin S J, Lee J, Park Y, Kim Y, Kim H and Choi J W 2022 Cationic additive with a rigid solvation shell for high-performance zinc ion batteries *Angew. Chem., Int. Ed.* **61** e202211589

[101] Lv Y, Zhao M, Du Y, Kang Y, Xiao Y and Chen S 2022 Engineering a self-adaptive electric double layer on both electrodes for high-performance zinc metal batteries *Energy Environ. Sci.* **15** 4748–60

[102] Hao R *et al* 2023 Reconstructing the solvation structure and solid-liquid interface enables dendrite-free zinc-ion batteries *Mater. Today Energy* **33** 101279

[103] Chen S *et al* 2019 Critical parameters for evaluating coin cells and pouch cells of rechargeable li-metal batteries *Joule* **3** 1094–105

[104] Cao Y, Li M, Lu J, Liu J and Amine K 2019 Bridging the academic and industrial metrics for next-generation practical batteries *Nat. Nanotechnol.* **14** 200–7

[105] Niu C, Lee H, Chen S, Li Q, Du J, Xu W, Zhang J-G, Whittingham M S, Xiao J and Liu J 2019 High-energy lithium metal pouch cells with limited anode swelling and long stable cycles *Nat. Energy* **4** 551–9

[106] Jain R, Lakhnot A S, Bhimani K, Sharma S, Mahajani V, Panchal R A, Kamble M, Han F, Wang C and Koratkar N 2022 Nanostructuring versus microstructuring in battery electrodes *Nat. Rev. Mater.* **7** 736–46

[107] Xiao P, Bu F, Zhao R, Aly Aboud M F, Shakir I and Xu Y 2018 Sub-5 nm ultrasmall metal-organic framework nanocrystals for highly efficient electrochemical energy storage *ACS Nano* **12** 3947–53

[108] Xiao P, Li S, Yu C, Wang Y and Xu Y 2020 Interface engineering between the metal-organic framework nanocrystal and graphene toward ultrahigh potassium-ion storage performance *ACS Nano* **14** 10210–8

[109] Piao Z, Xiao P, Luo R, Ma J, Gao R, Li C, Tan J, Yu K, Zhou G and Cheng H M 2022 Constructing a stable interface layer by tailoring solvation chemistry in carbonate electrolytes for high-performance lithium-metal batteries *Adv. Mater.* **34** e2108400

[110] Xiao P, Bu F, Yang G, Zhang Y and Xu Y 2017 Integration of graphene, nano sulfur, and conducting polymer into compact, flexible lithium-sulfur battery cathodes with ultrahigh volumetric capacity and superior cycling stability for foldable devices *Adv. Mater.* **29** 1703324

[111] Xiao P, Zhao Y, Piao Z, Li B, Zhou G and Cheng H-M 2022 A nonflammable electrolyte for ultrahigh-voltage (4.8 V-class) Li||NCM811 cells with a wide temperature range of 100 °C *Energy Environ. Sci.* **15** 2435–44

[112] Xiao P and Xu Y 2018 Recent progress in two-dimensional polymers for energy storage and conversion: design, synthesis, and applications *J. Mater. Chem.* A **6** 21676–95

[113] Wu Y and Liu N 2018 Visualizing battery reactions and processes by using in situ and in operando microscopies *Chem* **4** 438–65

[114] Ji Y *et al* 2021 From bulk to interface: electrochemical phenomena and mechanism studies in batteries via electrochemical quartz crystal microbalance *Chem. Soc. Rev.* **50** 10743–63
[115] Tripathi A M, Su W N and Hwang B J 2018 In situ analytical techniques for battery interface analysis *Chem. Soc. Rev.* **47** 736–851
[116] Zhang L, Qian T, Zhu X, Hu Z, Wang M, Zhang L, Jiang T, Tian J H and Yan C 2019 In situ optical spectroscopy characterization for optimal design of lithium-sulfur batteries *Chem. Soc. Rev.* **48** 5432–53
[117] Yang H, Tang P, Piao N, Li J, Shan X, Tai K, Tan J, Cheng H-M and Li F 2022 In-situ imaging techniques for advanced battery development *Mater. Today* **57** 279–94
[118] Yousaf M *et al* 2022 Visualization of battery materials and their interfaces/interphases using cryogenic electron microscopy *Mater. Today* **58** 238–74
[119] Wang Y, Liu Y, Song S, Yang Z, Qi X, Wang K, Liu Y, Zhang Q and Tian Y 2018 Accelerating the discovery of insensitive high-energy-density materials by a materials genome approach *Nat. Commun.* **9** 2444
[120] Liu Y, Guo B, Zou X, Li Y and Shi S 2020 Machine learning assisted materials design and discovery for rechargeable batteries *Energy Storage Mater.* **31** 434–50
[121] Burger B *et al* 2020 A mobile robotic chemist *Nature* **583** 237–41
[122] Deringer V L, Bernstein N, Csanyi G, Ben Mahmoud C, Ceriotti M, Wilson M, Drabold D A and Elliott S R 2021 Origins of structural and electronic transitions in disordered silicon *Nature* **589** 59–64
[123] Raccuglia P, Elbert K C, Adler P D, Falk C, Wenny M B, Mollo A, Zeller M, Friedler S A, Schrier J and Norquist A J 2016 Machine-learning-assisted materials discovery using failed experiments *Nature* **533** 73–76
[124] Correa-Baena J-P, Hippalgaonkar K, van Duren J, Jaffer S, Chandrasekhar V R, Stevanovic V, Wadia C, Guha S and Buonassisi T 2018 Accelerating materials development via automation, machine learning, and high-performance computing *Joule* **2** 1410–20
[125] Nolan A M, Zhu Y, He X, Bai Q and Mo Y 2018 Computation-accelerated design of materials and interfaces for all-solid-state lithium-ion batteries *Joule* **2** 2016–46
[126] Xiao Y, Miara L J, Wang Y and Ceder G 2019 Computational screening of cathode coatings for solid-state batteries *Joule* **3** 1252–75
[127] Butler K T, Davies D W, Cartwright H, Isayev O and Walsh A 2018 Machine learning for molecular and materials science *Nature* **559** 547–55